Basin Research

IAS EAGE

Basin Research (2018) **30** (Suppl. 1), 289–310, doi: 10.1111/bre.12221

Chronology of Chilean Frontal Cordillera building from geochronological, stratigraphic and geomorphological data insights from Miocene intramontane-basin deposits

Katia Rossel,*, † Germán Aguilar,*, † Esteban Salazar,‡ Joseph Martinod,§ Sébastien Carretier,¶ Luisa Pinto* and Albert Cabré**

*Departamento de Geología, Facultad de Ciencias Físicas y Matemáticas, Universidad de Chile, Santiago, Chile

†Facultad de Ciencias Físicas y Matemáticas, Advanced Mining Technology Center, Universidad de Chile, Santiago, Chile

‡Servicio Nacional de Geología y Minería, Santiago, Chile

§ISTerre, Université de Savoie-Mont Blanc, Le Bourget-du-Lac, France

¶IRD Géosciences Environnement Toulouse, Toulouse, France

**Programa de Doctorado en Ciencias Mención Geología, Universidad Católica del Norte, Antofagasta, Chile

ABSTRACT

The Chilean Frontal Cordillera, near 28°45′S, provides a remarkable example to explore the evolution of the Central Andes; this area provides conspicuous pediment surfaces and continental deposits, which allowed us to analyse the timing and propagation of deformation which controlled the Andes building during the Cenozoic using structural, geomorphological, sedimentological, stratigraphic and geochronological data. The study area is characterized by outcrops of the Cerro del Burro Gravels, a continental deposit which is surrounded by four morphostructural mountain systems. Based on a 46 Ma tuff affected by a syncline, which is sealed by a 44 Ma tuff, we recognized an Eocene fault activity that contributed to the uplift of the western and northern systems, which have remained inactive during the last 44 Ma. The deformed lithologies during the last pulse of activity of the western fault and the youngest lithology carved by pediment processes (21 Ma) indicate a pediment surface developed during the Late Eocene and Oligocene. This pediment extended below the Cerro del Burro Gravels associated to a base level which drained to the east. We also recognized Miocene fault activity that played a main role in the uplift of the eastern and southern systems. Geochronological, stratigraphic and geomorphological data suggest a first pulse of fault activity between 19 and 13 Ma, which interrupted the pedimentation processes, developed an intramontane depocenter, and forced the accumulation of the Laguna Grande Succession in an alluvial-braided fluvial environment. After 13 Ma, an erosive event evidenced by the incision of valleys, resulted after the change in the extension and configuration of the hydric network.

INTRODUCTION

The evolution of the western margin of South America in Northern Chile and Argentina has been governed by a generalized subduction regime since the Jurassic (Coira *et al.*, 1982). Nevertheless, the growth of the Andean orogen started during the Late Cretaceous and occurred during several discrete episodes of crustal thickening separated by periods of tectonic quiescence and/or extension (Steinman, 1929; Charrier *et al.*, 2007). Since the Late Cretaceous, crustal thickening in the Central Andes resulted in uplift and progressive widening of the chain (Gubbels *et al.*, 1993; Armijo *et al.*, 2015). To explain this late (compared to the long history of oceanic subduction) and episodic growth of the Cordillera, it has been proposed that the phases of tectonic shortening occurred either during periods of rapid and orthogonal convergence between South America and the subducting plate (Pardo-Casas & Molnar, 1987; Charrier *et al.*, 2009), or during periods of rapid absolute westward motion of the South American continent (Silver *et al.*, 1998; Sobolev & Babeyko, 2005). Another factor that may also constrain the intensity and location of continental shortening is the geometry of the slab, possibly affected by the subduction

Correspondence: Germán Aguilar, AMTC-FCFM, Universidad de Chile. Tupper 2007, Post Code: 8370451, Santiago, Chile. E-mail: german.aguilar@amtc.cl

of topographic disruptions (e.g., Pilger, 1984; Yáñez *et al.*, 2001; Espurt *et al.*, 2008). Horizontal slab segments may favour both an increase in the continental shortening, and the migration of shortening within the continental plate (e.g., Gutscher *et al.*, 2000; Ramos *et al.*, 2002; Martinod *et al.*, 2010; Ramos, 2010).

During the widening of an orogen, foreland areas are incorporated as intramontane basins, which are filled with sediments as their base level disconnects from the foreland (Sobel *et al.*, 2003; Ballato *et al.*, accepted). This process has been largely studied on the eastern side of the Central Andes that constrain the eastward migration of the orogene (Sobel *et al.*, 2003; Strecker *et al.*, 2009). In contrast, the eastward migration is poorly documented on the present-day western slope of the Andes. In this article, we analyse the tectonic, sedimentary and geomorphological evolution of an intramontane basin situated in northern Chile close to 28°45′S, above the northern part of the present-day Chile-Argentina flat-slab segment. The gravels that fill the studied basin are known as the Cerro del Burro Gravels, and have only been studied at a regional scale (Reutter, 1974; Nalpas *et al.*, 2009; Moscoso *et al.*, 2010). The geological and geomorphological evolution of each morphostructural system conforming the study area and its records (erosion, gravel deposits, development of low relief surfaces) can help to unravel the tectonic history of the basin and therefore can contribute to understand the mechanisms and timing involved in the Cenozoic construction of the Andes. With this aim, we present a morphostratigraphic analysis of gravel successions, the paleoenvironment in which these series deposited, and analyse the sedimentary provenance of sediments taking into account grain counting of sands and geochronological data of their U-Pb detrital zircons.

Geodynamic setting

The continental shortening responsible for the growth of the Andean Cordillera has been attributed to the final break-up of Western Gondwana, the opening of the South Atlantic Ocean, and the beginning of the westward drift of South America in the hot-spot reference frame (e.g., Ramos, 2010). Following this, the Andean margin has been subject to several discrete episodes of crustal thickening (the so called tectonic phases), separated by periods of tectonic quiescence and/or extension (Steinman, 1929; Charrier *et al.*, 2007). The first two phases correspond to the Peruvian and K-T orogenies, which are recognized along the present day Coastal Cordillera and in the western margin of the Frontal Cordillera, respectively (Charrier *et al.*, 2007; Salazar *et al.*, 2013; Martínez *et al.*, 2016). During the Eocene a compressive event took place in the Central Andes (the "Incaic" phase; Steinman, 1929; Jaillard & Soler, 1996; Lamb *et al.*, 1997). Later on, during the late Oligocene-late Miocene, the Andean margin was affected by the "Pehuenche" compressive phase (Yrigoyen, 1993), which has been related to the "Quechua phase" identified further north (Steinman, 1929; Salfity *et al.*, 1984; Charrier *et al.*, 2009). This episode of crustal shortening has been attributed to the sudden change in the subduction parameters, the obliquity and velocity, following the rupture of the Farallon plate. The end of this episode is associated to the beginning of the relief incision in the forearc in the western slope of the Andes (Charrier *et al.*, 2009). Between the Incaic and Pehuenche phases, the area along 30–36°S was controlled by a generalized extensional regime (Charrier *et al.*, 2007, 2009; Winocur *et al.*, 2014).

The area studied in this work is located above the Chilean flat-slab region (27–34°S; Fig. 1), where the Nazca Plate is subducting subhorizontally beneath the South American Plate (Barazangi & Isacks, 1976). Such configuration has been attributed to the subduction of the Juan Fernández Ridge during the Neogene (Yáñez *et al.*, 2001). Petrological and geochemical studies, as well as geodynamic reconstructions, suggest that between 12 and 10 Ma the ridge arrived to the northern part of the flat-slab region (Kay *et al.*, 1988; Yáñez *et al.*, 2001; Kay & Mpodozis, 2002). After the beginning of ridge subduction, a significant decrease in the volcanic activity has been observed in the region (Bissig *et al.*, 2002; Kay & Mpodozis, 2002). The end of arc volcanism occurred 5 Ma ago (Bissig *et al.*, 2002; Kay & Mpodozis, 2002; Ramos *et al.*, 2002), indicating a delay of 7 Ma between the beginning of ridge subduction and the configuration of the present day flat-slab (Espurt *et al.*, 2008). In addition, the development of the flat subduction also determined the propagation of the deformation front to the east (Ramos *et al.*, 2002; Charrier *et al.*, 2007; Espurt *et al.*, 2008; Martinod *et al.*, 2013). The Pliocene and Pleistocene crustal shortening was restricted to the Sierras Pampeanas and the Precordillera in Argentina (Allmendinger *et al.*, 1983; Jordan *et al.*, 1983; Ramos *et al.*, 2002), nearly 200 km eastwards from the subduction margin (Fig. 1; Pardo *et al.*, 2002).

Local geology

The study area is located within the Frontal Cordillera (Fig. 1), a series of NS thrusting belt that expose Late Paleozoic basement trending blocks of crystalline basement unconformably covered by Mesozoic and Cenozoic strata (Fig. 2). The crystalline basement is made up of granitic plutons, grouped in the Chollay Plutonic Complex (Lower-Middle Triassic) intruding the Permian volcaniclastics and Devonian metasediments of the Las Placetas Formation (Salazar *et al.*, 2013; Salazar & Coloma, Accepted). The Mesozoic cover is comprised by the dacitic to andesitic volcanics of the Guanaco Sonso and the La Totora formations (Middle to Upper Triassic); the marine limestones and sandstones of the Lautaro Formation (Lower to Middle Jurassic); the alluvial siliciclastics of the late Jurassic Lagunillas Formation (Early to Middle Jurassic; Mora, 2014); and fluvial to alluvial siliciclastic of the Pucalume Formation (Upper Cretaceous; Salazar & Coloma, Accepted). The Cenozoic cover in the

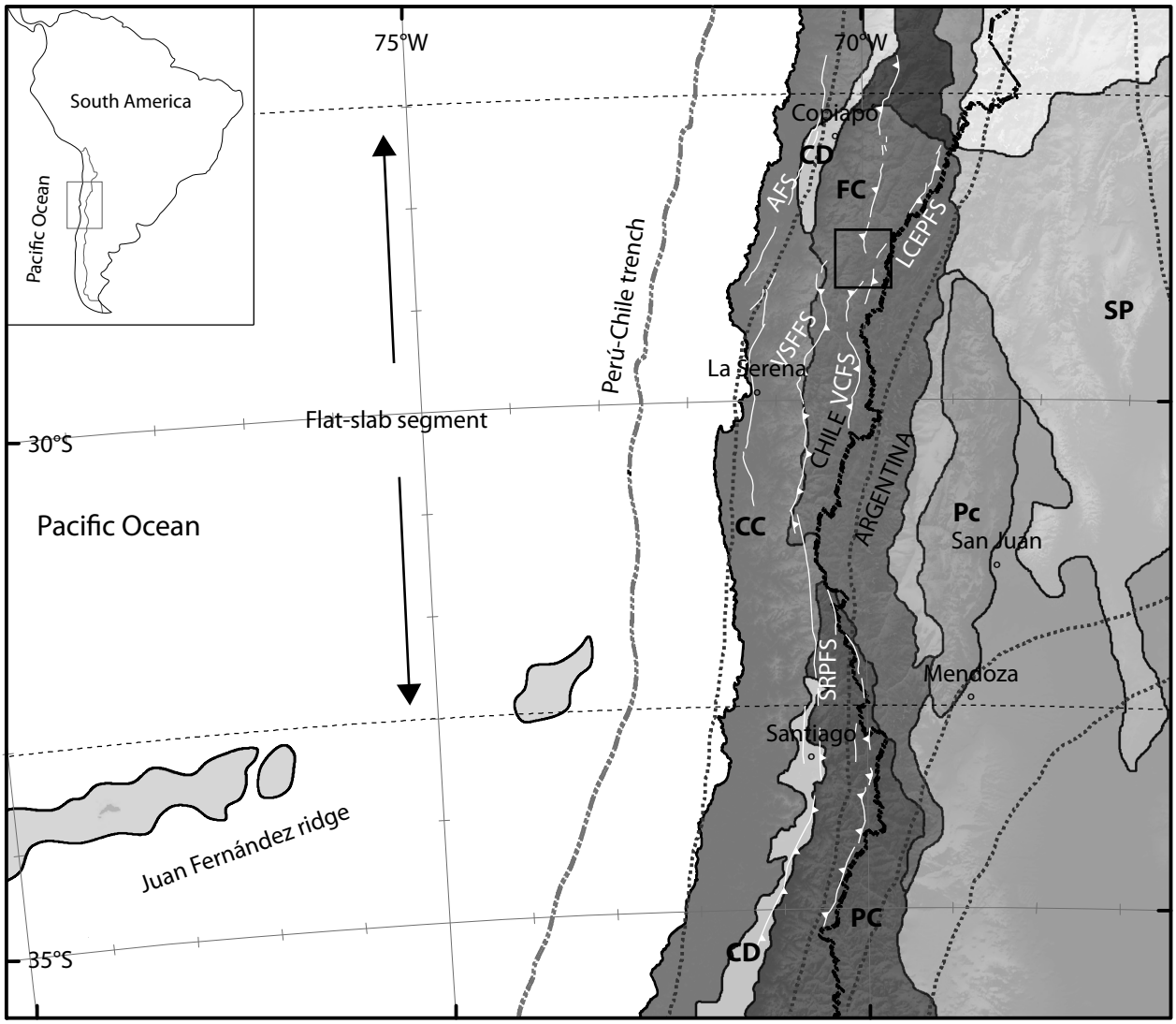

Fig. 1. Morphostructural units and tectonic configuration of the Central Andes. CC, Coastal Cordillera; FC, Frontal Cordillera; CD, Central Depression; DR, Domeyko Range; Pc, Precordillera; PC, Principal Cordillera; SP, Sierras Pampeanas; AP, Altiplano-Puna. White lines show main faults: AFS, Atacama Fault System; VSFFS, Vicuña-San Félix Fault System; Valeriano-Chollay Fault System; LCEPFS, La Coipa-El Potro Fault System; SRPFS, San Ramón-Pocuro Fault System. Black box shows the location of the studied area. Black dotted lines indicate the geometry of the Wadati-Benioff zone as contours of depth, according to Cahill & Isacks (1992). Black segmented line shows the international limit between Chile and Argentina. Image modified from Charrier *et al.* (2007) and Rodríguez *et al.* (2014); faults extracted from Salazar *et al.* (2013); Creixell *et al.* (2013), Jara & Charrier (2014) and Contreras & Schilling (2012).

area includes the siliciclastic and volcaniclastic rocks of the Quebrada Seca Formation (Paleocene; ca. 63 Ma, Fig. 2); an Eocene volcanic and intrusive complex located at the northwest corner of the study area (The El Gaucho beds and the Tres Morros Plutonic Complex); alluvial siliciclastics to the east (Manflas Beds) and the volcanics of the Escabroso Formation, of ca. 21 Ma, in the eastern half of the study area (Salazar & Coloma, Accepted). The semi consolidated Cerro del Burro Gravels (CBG) is unconformably deposited above these series (Moscoso *et al.*, 2010). Further details of this gravel deposit are presented in the next section.

The structural style of the study area is controlled by the uplift of four morphostructural systems through bivergent reverse faults (Salazar & Coloma, Accepted) that surround the main Miocene depocenter (Fig. 2). The western system was uplifted by the east vergent Valeriano Fault. This fault is sealed by the Laguna Grande Succession and deforms a Paleocene volcanic sequence in a footwall syncline, which constrains its activity between 63 and 21 Ma. (Fig. 3a). The hanging wall of this major fault is composed or Permo-Triassic basement and Mesozoic rocks, all unconformably covered by the Eocene El Gaucho beds, indicating an Eocene uplift of this system. This fault does not present any morphological expression. The northern morphostructural system was uplifted by two opposite vergent reverse faults (Fig. 4), which generated a wide anticline in the Mesozoic to Eocene strata.

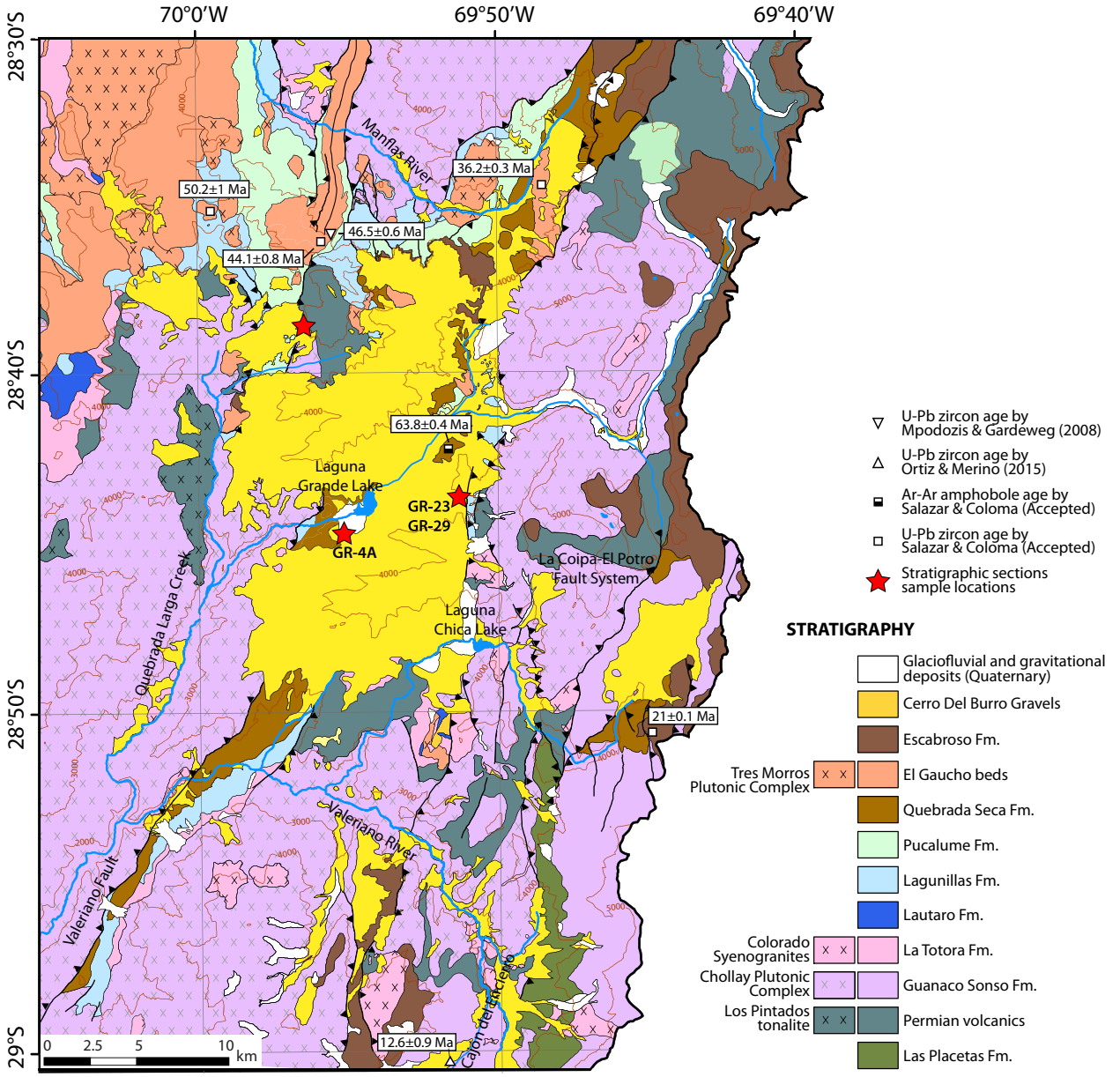

Fig. 2. Geological map of the Laguna Grande Lake area. Red stars show the location of the outcrops described in this work, and white triangles and rectangles show the U-Pb zircon ages reported by Ortiz & Merino (2015) and Salazar & Coloma, Accepted, respectively.

This structure is unconformably covered by ca. 21 Ma volcanic rocks and by the CBG (Fig. 2). Additionally, an internal tight syncline within this uplifted relief affects a 46 Ma tuff and is sealed by another 44 Ma tuff (Fig. 3b; Mpodozis & Gardeweg, 2008; Salazar & Coloma, Accepted), thus defining the age of last pulse of deformation to the Eocene. The eastern morphostructural system was uplifted by a series of west-vergent reverse faults grouped in the La Coipa-El Potro Fault System (Salazar & Coloma, Accepted; Fig. 2) which extends approximately for 200 km. This fault system is characterized by a thick-skinned deformation style that uplifts deep basement blocks over the Cerro del Burro Gravels (Salazar & Coloma, Accepted). The southern morphostructural system was uplifted mainly by west vergent reverse faults (Salazar & Coloma, Accepted).

METHODOLOGIES

Geomorphological analysis

In the study area, low relief surfaces (slope <20° and relief <600 m) define several pediment relicts in the watersheds interfluves of the morphostructural systems and terraces in the slope of valleys (Bissig *et al.*, 2002; Aguilar *et al.*, 2011; Rossel, 2014). These surfaces were mapped based on field observations, using a morphometric data extracted from a digital elevation model, where we evaluate elevation and slope (SRTM, ~90 m of pixel size), and observations of Google Earth images. We also mapped the contact between the CBG and the basement to obtain an approximation of the surface below these gravels. This was done based on field observations, and using a series of

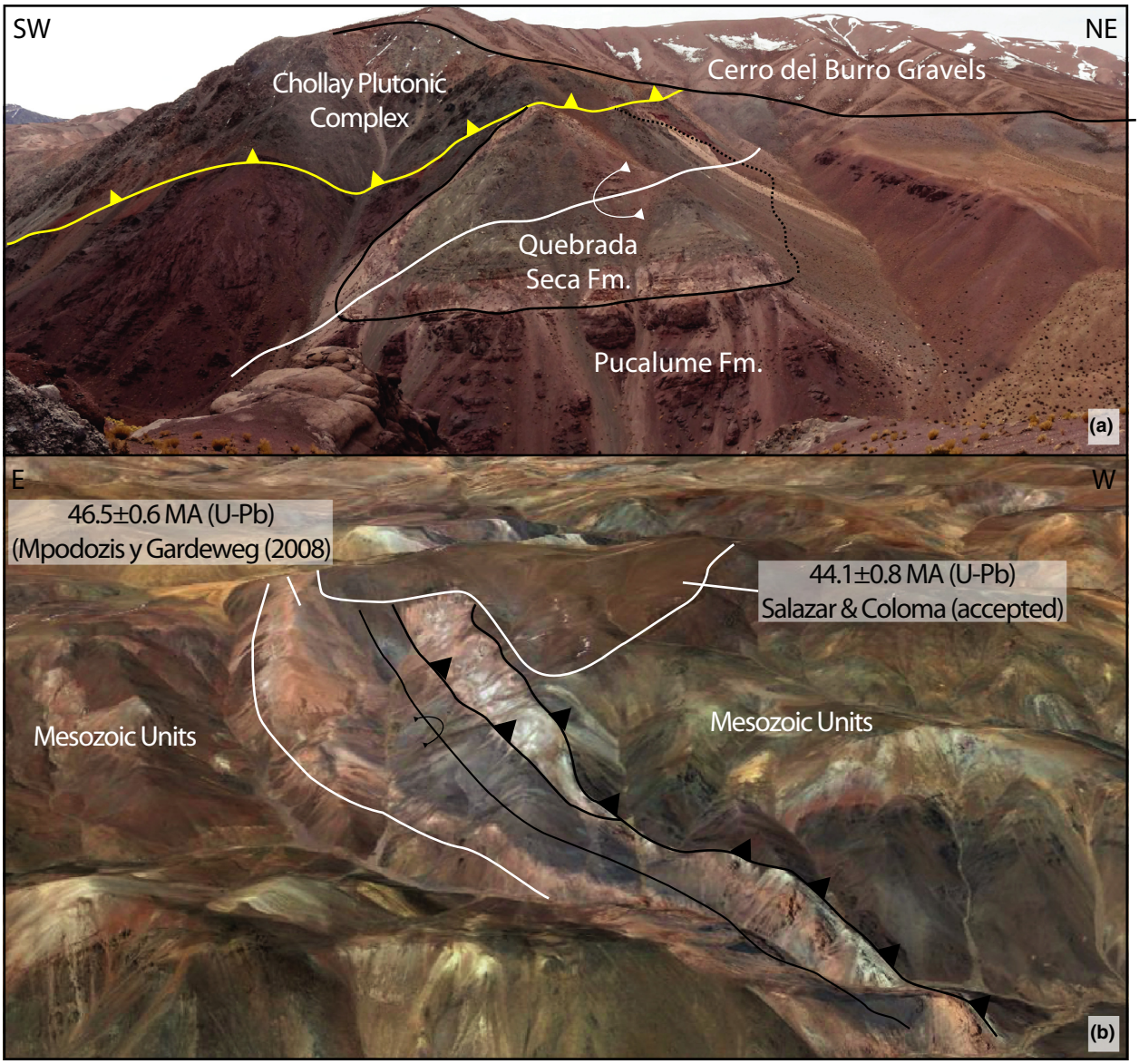

Fig. 3. Photographs showing Eocene deformation recognized in the study zone. (a) NW view, showing the deformed Paleocene Quebrada Seca Formation, overlain by Permo-Triassic basement uplifted by the Valeriano Fault, which in turn is covered by the CBG; (b) S view showing the internal syncline affecting a 46 Ma tuff, which is sealed by a 44 Ma tuff.

ASTER RGB band combinations. Subsequently, the contact and the low relief surfaces were interpolated, separately, using the Natural Neighbour method (Sambridge *et al.*, 1995). This allowed us to reconstruct the current geometry of the paleotopography before the deposition of the CBG and also the surface that represents to the top of this deposit.

Depositional environment and sedimentary provenance

In order to establish the depositional environment of the Cerro del Burro Gravels (CBG), we carried out a comprehensive sedimentological and stratigraphic study. Three outcrops were studied in detail during field work (Fig. 2), where three stratigraphic columns were constructed and a series of lithofacies were defined, following the facies code of Miall (1996) and Horton & Schmitt (1996).

The composition of sediments was analysed during field work and on 9 thin sections extracted from sand lens and sand matrix of gravels. We also performed a provenance analysis using the Gazzi-Dickinson point count method developed independently by Gazzi (1966) and Dickinson (1970). This method minimizes variation in composition with grain size, thus eliminating the need for sieving and multiple counts of different size fractions (Ingersoll *et al.*, 1984). Three hundred points were counted per section, using the maximum grid spacing that resulted in coverage of the entire slide section, which yielded statistically reliable values for all parameters (Van der Plas & Tobi, 1965). Matrix and cement were not counted (Ingersoll *et al.*, 1984).

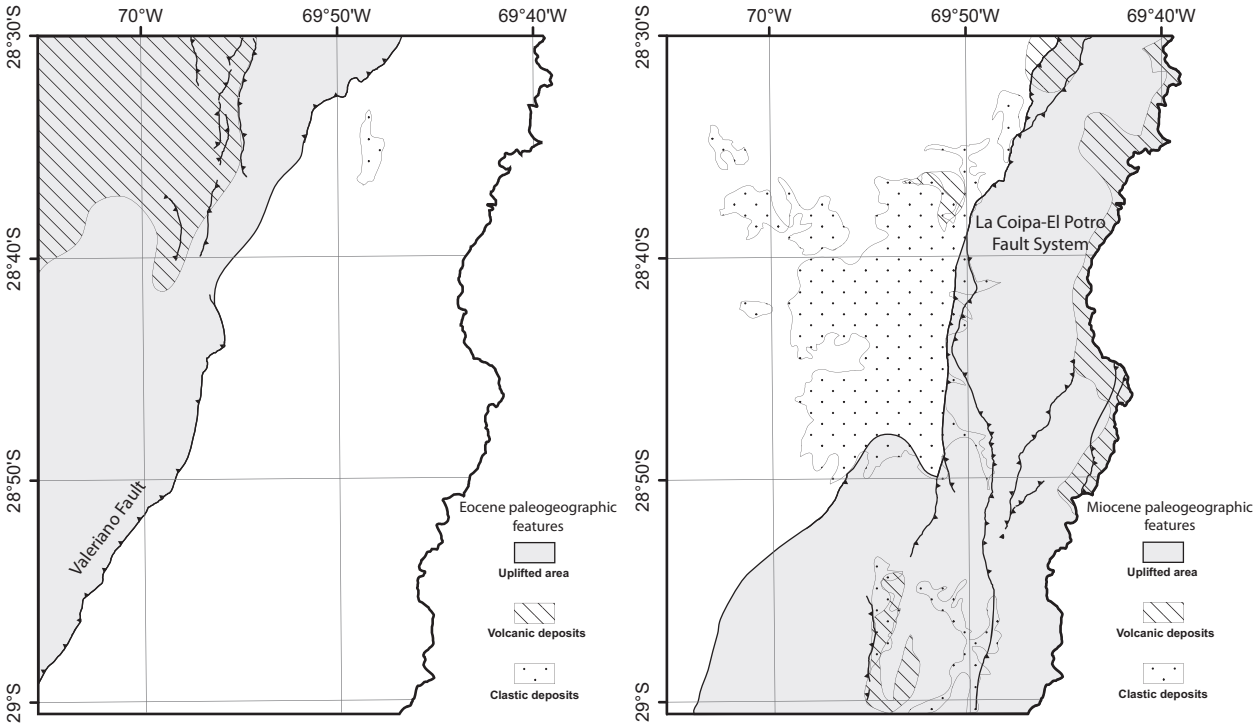

Fig. 4. Simplified map, showing active structures and uplifted areas: (a) Eocene faults and N and NW mountain system uplifted by these structures. Volcanic and clastic deposits developed during Eocene are also shown; (b) Miocene faults, which uplifted the E and S mountain system. Volcanic and clastic deposits developed during Miocene are also presented.

Age determinations in zircons were performed in three samples (see Table S1, Table S2 and Table S3 of Appendix S1) in order to obtain a better understanding of the geological framework for the gravels deposition. We also performed a morphological study of zircons through cathodoluminescence (CL) images to improve the selection of crystals and points of determinations and helping to establish their origin, as intrusive or extrusive.

Zircons separation and U-Pb detrital zircon analysis were performed in the Chilean Geological Survey (Servicio Nacional de Geología y Minería). Zircons separation was done using standard mineral separation techniques. After crushing and sieving, zircon grains were separated using a Gemini Table, a Frantz magnetic separator and heavy liquids (bromoform and methylene iodide). Final zircon selection was achieved by hand-picking using a binocular microscope. For U-Pb analyses, zircon grains were firstly mounted in an epoxy resin that was polished to expose the grains. U-Pb analyses were conducted by laser ablation inductively coupled plasma mass spectrometry (LA-ICP-MS; Servicio Nacional de Geología y Minería) in a Thermo Fischer Element XR spectrometer with a Photon-machines Analyte G2 laser.

Detrital zircon age diagrams were elaborated using the geochronological toolkit Isoplot (Ludwig, 2003) and the age peaks were determined using the Excel macro Agepick program (Gehrels, 2009). To determine the source of each zircon, Th/U rates were plotted, following the parameter defined by Rubatto (2002). Determinations with discordance over 25% or reverse discordance over 5% were considered unreliable and were not used. Analyses with an error greater than 10% were also excluded. For further details of U-Pb determinations see the Appendix.

RESULTS

Geomorphology

In the study area, several low relief surfaces were recognized. In the western morphostructural system is recognized an extending erosive low relief surface (Figs 5 and 6a), called the Las Pintadas Surface. This surface tilts to the south and east, with elevations between 3.2 and 4.5 km a.s.l. and between 1.6 and 0.8 km above the bottom of the main present-day valley. To the east, this surface is covered by the Cerro del Burro Gravel (CBG) deposit (Figs 5 and 6a). The interpolated contact between the gravels and the bedrock indicates the continuity to the east of the smooth covered erosive surface. This surface shows a southward average slope of 5°, being generally less than 10°, and is between 0.2 and 0.6 km above the bottom of the main valley. The interpolation also shows a bedrock high, to the north, which limits the basin. Such higher bedrock corresponds to the Eocene structure that uplifted the northern morphostructural system (Figs 4a and 5). Large outcrops of Permo–Triassic rocks have been carved by the Las Pintadas Surface, as well as volcanic Eocene to lower Miocene successions, indicating a long-term evolution of this pediment surface, which developed until Miocene.

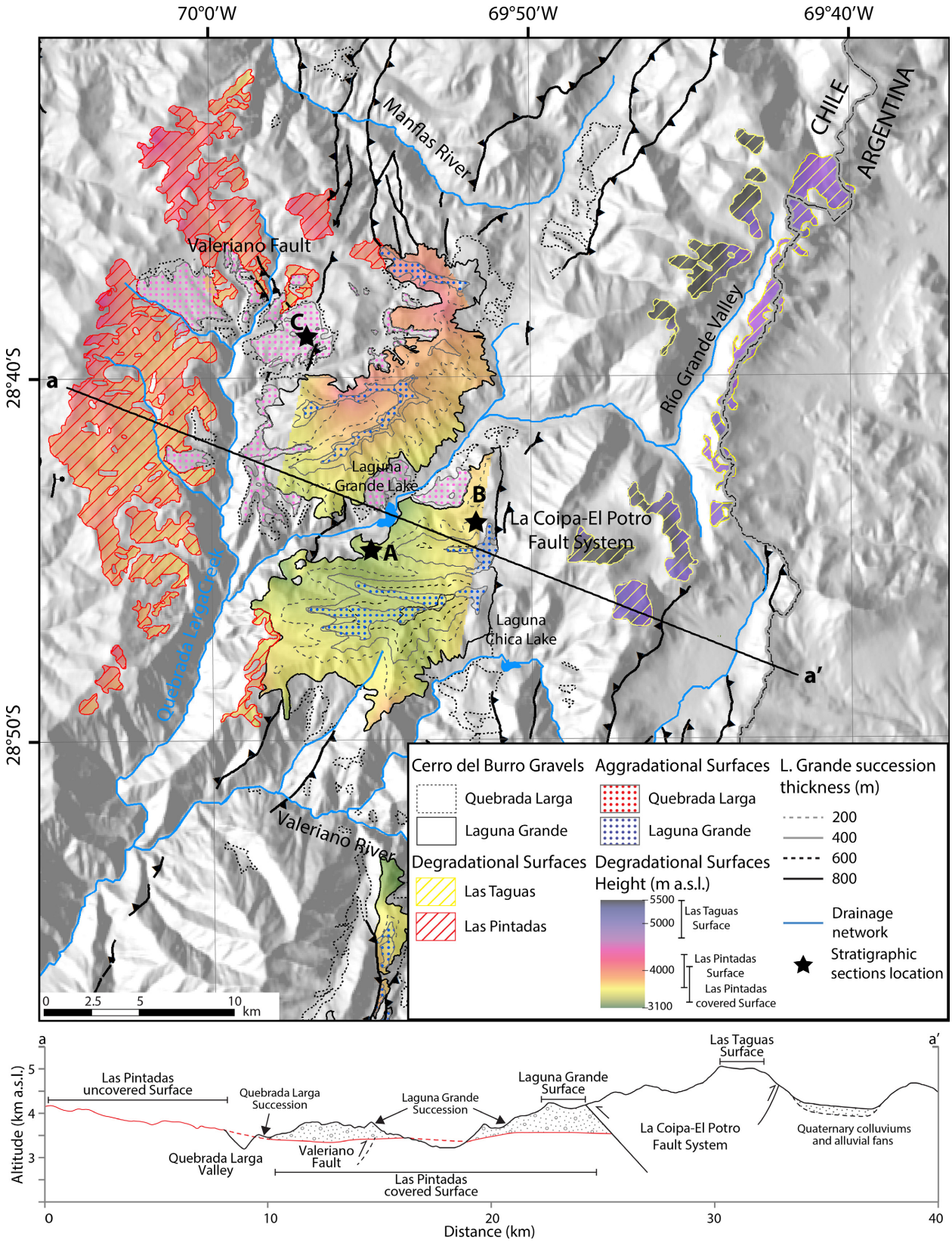

Fig. 5. Shaded relief map with the Las Pintadas Surface, the interpolation of the covered surface under the gravel deposit (covered Las Pintadas Surface) and the Las Taguas Surface. Colours represent the height of these two degradational low relief surfaces. Black stars show the location of the outcrops described in this work. CBG are presented with different contours that indicate independently the two successions of gravels. Aggradational surfaces associated to each gravels succession are also shown. Section a–a' presents the surfaces locations and heights. Surfaces have been disturbed by faults activity and incision. This section also shows the Las Pintadas Surface and its continuation below the gravels (red line).

The top of the gravels deposit defines the aggradational Laguna Grande low relief surface. This surface is only preserved from erosion in the interfluves between the Laguna Grande and Laguna Chica lakes (Figs 5 and 6a). The altitude of this aggradational surface varies between 3.6 and 4.4 km a.s.l., which is between 1 and 1.4 km above the bottom of the main valley. The distribution of gravel thickness reveals a major accumulation to the south with up to 840 m and a progressive northward decrease up to 400 m (Fig. 3).

Low relief surfaces and gravel deposits are interrupted by the La Coipa-El Potro Fault System, which uplifts the eastern morphostructural unit (Figs 4b and 5). In this system, erosive low relief surfaces are only preserved in the interfluves. These surfaces, grouped in the Las Taguas Surface (Fig. 5), are between 4.9 and 5.4 km a.s.l., which is between 1.7 and 2.2 km above the bottom of the main valley. As the Las Pintadas Surface, this surface has been carved in lower Miocene volcanic successions (Fig. 2), but it does not have a gravel cover. Therefore, we propose that the Las Taguas surface corresponds to the eastern extension of the Las Pintadas Surface, uplifted by the La Coipa-El Potro Fault system. These observations indicate that the paleogeography and the evolution of the CBG depocenter has been controlled by the uplift of the eastern morphostructural system.

Along the slopes of the main valley, the Las Pintadas Surface has been exhumed and partially covered by reworked gravels. The exhumed surface was affected by geomorphic processes, forming terraced and talus flatiron, which define the Quebrada Larga Surface (Figs 6b–d). Upstream of the valley, this surface progressively disappears and the gravels are reworked by quaternary colluviums and alluvial fans (Fig. 6e), which construct the terraces near of valley bottom, only eroded by the most recent incision (Aguilar, 2010).

Facies associations and depositional environments

The Cerro del Burro Gravel (CBG) deposit is composed mainly of polymictic coarse clast and matrix supported gravels with intercalations of lenticular and tabular sands (Rossel, 2014). Two distinct successions were defined separated by erosional unconformities and correlated with the previous geomorphologic analysis of low relief surfaces. These, from older to younger, have been grouped in the Laguna Grande and Quebrada Larga successions (Figs 5 and 6). The 21 Ma dacitic tuff under the Laguna Grande Succession and the 13 Ma tuff intercalated with the Quebrada Larga Succession allowed us to constrain the deposition age for the CBG deposit (Fig. 2).

Laguna grande succession

The Laguna Grande Succession corresponds to the thickest deposit, which overlays a 21 Ma dacitic tuff and basaltic flows. This succession occurs in a topographical N-S trending depression flanked by uplifted morphostructural systems configuring an intramontane basin (Fig. 2). As described before, the depression is flanked to the west by Eocene structures. To the east, some of the recognized faults cut the Laguna Grande deposits, suggesting a Miocene to present activity (Fig. 4b). The thickest outcrop of the Laguna Grande Succession (column A; ~300 m) is exposed next to the Laguna Grande Lake (Fig. 2). In this location, although the same lithofacies were identified along the section, a general vertical variation on their distribution is observed.

The basal part (0–150 m) of the succession consists of thick series of stratified, clast-supported and unsorted gravels showing sub-rounded to sub-angular clasts, with diameters up to 0.8 m, in a matrix composed of medium to coarse sand. These series are inferred to represent clastic rich debris flow deposits (facies Gci, Gcn and Gcm; Table 1; Figs 7 and 8). Subordinately, matrix-supported unsorted gravels (facies Gmm and Gmg), interpreted as pseudoplastic debris flow deposits, are intercalated within the clast-supported facies. Both clast- and matrix-supported gravels occur as tabular layers that vary laterally to decimetric to metric fillings of previously carved channels (Fig. 7a1 and a2), representing the backfilling stages on the cyclic evolution of the alluvial system (Schumm *et al.*, 1987). Massive decametric tabular and lenticular shaped beds, with erosional bases of medium to coarse sands (facies Sm), are inter-fingered with the debris flow deposits. These are inferred to represent stream and flood flows desiccated, and channel infill facies, respectively, suggesting a shallow braided system. Such systems are developed widely on the "dispersion" stages of the cyclic evolution of an alluvial fan system, and are usually linked to the release of an entrenched flow, whether from the main feeder canyon or by the generation of a distal depositional lobe (Schumm *et al.*, 1987; DeCelles *et al.*, 1991). The basal section also contains minor centimetric intercalations of silt and mud with occasional desiccation cracks, which are interpreted as overbank and abandoned channel deposits (facies Fm). Finally, discrete levels of carbonate indurated strata occur within the sandy matrix of gravels (facies P), which are interpreted as carbonated paleosols revealing periods of relative stability and hiatus in the deposition. The observed facies in this basal section suggest a proximal alluvial fan environment dominated by aggrading debris flow deposits with important coarse sediment supply in a dry environment.

The upper part (150–300 m) of the Laguna Grande Succession is also made up of debris flow deposits, but it is dominated by the stacking of matrix-supported gravels (facies Gmm and Gmg; Figs 7 and 8). The clasts and matrix are similar in composition to the basal member but the matrix is more abundant and block diameters reach up to 1.2 m. Massive parallel and tabular strata

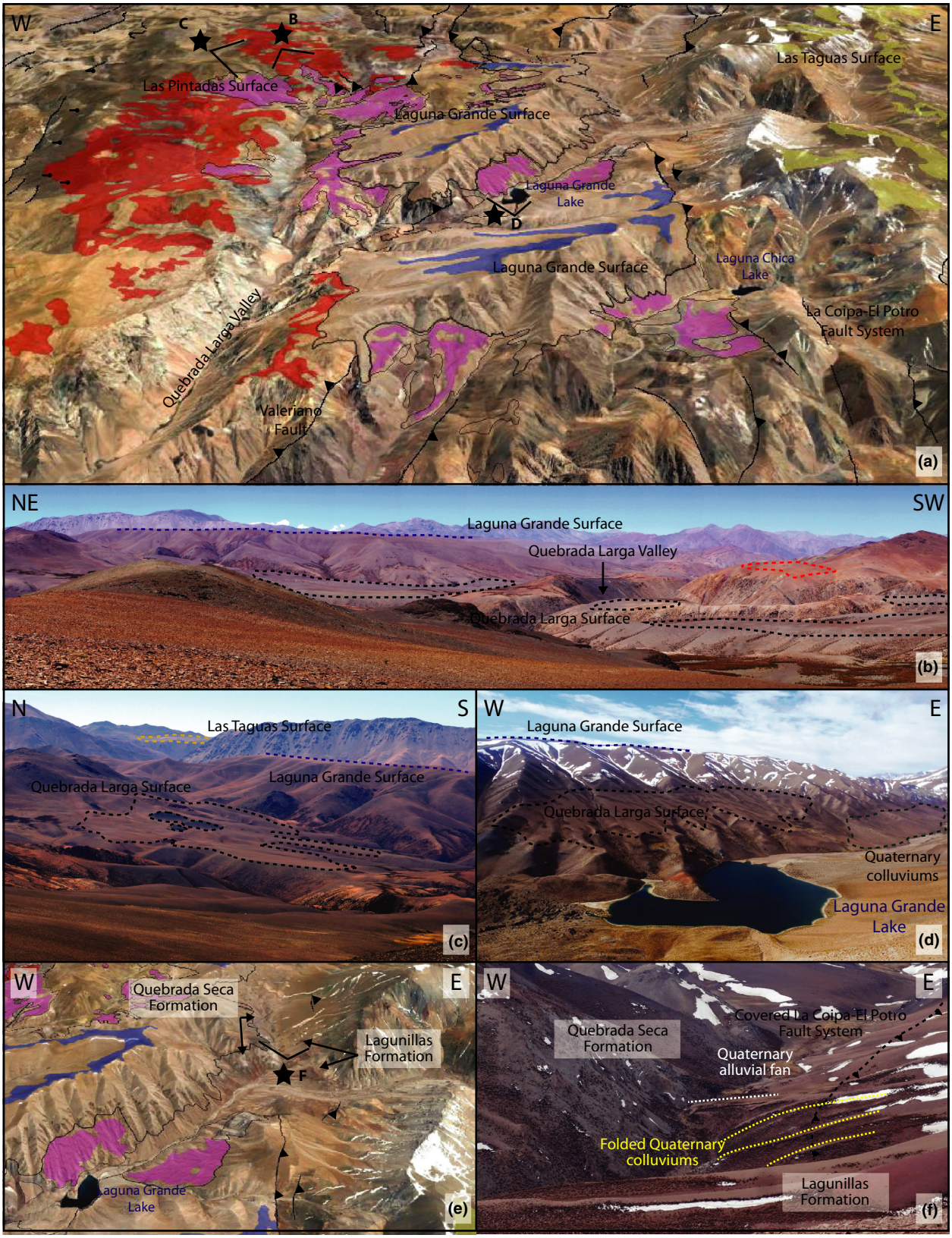

Fig. 6. (a) 3-D oblique GoogleEarth view showing the following surfaces: Las Pintadas (red), Las Taguas (yellow), Laguna Grande (blue), Quebrada Larga (pink), Los Tambillos (green). Black stars show the locations from where photographs b, c and d were taken. (b) NW view showing the relation between the Las Pintadas, Laguna Grande and Quebrada Larga surfaces. (c) E view towards the eastern mountain system, showing the Las Taguas, Laguna Grande and Quebrada Larga surfaces. (d) N view showing the relation between aggradational surfaces. (e) Oblique 3-D display (GoogleEarth) showing approximate location of photograph f; (f) N view of the Los Tambillos Succession folded by the La Coipa-El Potro Fault System.

Table 1. Description of the observed lithofacies. Facies based on Miall (1996)

Code	Facies	Description	Depositional processes
Gmm	Matrix supported, massive gravels	Sub-angular to sub-rounded, ungraded gravels, in a sandy matrix.	Plastic debris-flow (Miall, 1996).
Gmg	Matrix supported gravels	Sub-angular to sub-rounded, inverse to normal grading gravels, in a sandy matrix.	Pseudoplastic debris-flow (Miall, 1996).
Gci	Clast supported, inversely graded gravels	Sub-angular to sub-rounded gravels, showing inverse grading.	Clastic rich debris flow or pseudoplastic debris flow (Miall, 1996).
Gcn	Clast supported normally graded gravels	Sub-angular to sub-rounded gravels, showing normal grading.	Hyper-concentrated flow, high-density turbidity currents (Horton & Schmitt, 1996).
Gcm	Clast supported, massive gravels	Sub-angular to sub-rounded, ungraded gravels, in a sandy matrix.	Plastic or pseudoplastic debris-flow (Miall, 1996).
Gpt	Planar and trough cross-stratified gravels	Matrix supported gravels with trough and planar cross-beds.	Minor channel fills, transverse bedforms, deltaic growths from older bar remnants (Miall, 1996).
Spt	Planar and trough cross-stratified sand	Planar and trough crossbedded sands	Lower-flow-regime conditions (Miall, 1996).
Sm	Massive sand	Unstratified fine to coarse sand.	Subaereal waning flood flows (Horton & Schmitt, 1996) and desiccation.
Fm	Mud, silt	Massive mud with desiccation cracks.	Overbank, abandoned channel or drape deposits (Miall, 1996).
P	Paleosol carbonate	Indurated carbonate strata.	Soil with chemical precipitation (Miall, 1996).

and lenticular shapes of sands (facies Sm) are more abundant than in the base of the succession. Thinner to medium lens of clast-supported gravels are interfingered with the matrix-supported gravels. Carbonate cemented strata (facies P) are also present. These facies also suggest a proximal alluvial fan environment, although the increased abundance of clast-poor debris flows suggests a more evolved stage than that from the basal section (Blair & McPherson, 1994).

To the east of the column previously described, another outcrop (~150 m) of the Laguna Grande Succession was studied near a trace of the La Coipa-El Potro Fault System (Fig. 2). The upper part of the succession (~500 m thick) is covered by modern colluvial deposits and is not exposed. The remaining parts consists almost exclusively of matrix-supported gravels (facies Gmm and Gmg) inter-fingered with a few thinner lenticular sands (facies Sm) and clast-supported medium gravels (facies Gci, Gcn and Gcm; Figs 7b1, b2, and 8). The diameter of blocks reaches up to 1.2 m and clasts and matrix are similar in composition to the western succession. Carbonate strata (facies P) are persistently present throughout the entire succession, reflecting hiatuses during the deposition. The eastern column correlates well with the upper member of the western column but the abundant sandy facies suggests a more distal position to the east (Blair & McPherson, 1999). However, more subangulous clasts are observed in the eastern column, as well as brownish less dense and disaggregated beds, indicating load casts, which were not present in the other outcrops. These clasts and load casts suggest a contribution from a nearby source, probably from the east, from the block uplifted by the La Coipa-El Potro Fault System.

Quebrada larga succession

The Quebrada Larga Succession outcrops surrounding the Laguna Grande Succession, in a lower elevation, but several meters above the current valleys (~300 m). Most of the Quebrada Larga Succession are recognized along the Quebrada Larga Creek and near the Laguna Grande and Laguna Chica Lakes (Fig. 5). Minor deposits in the Cajón del Encierro have a ca. 13 Ma Dacitic tuff intercalated near its base (Fig. 2; Ortiz & Merino, 2015), which represents the maximum age of this succession and a minimum age for the deposition of the Laguna Grande Succession.

The studied column for the Quebrada Larga Succession (~90 m) is located near the head of the homonymous river (Fig. 2). This succession includes thick layers of massive and cross-bedded sands (facies Spt and Sm; Fig. 7c2), minor intercalations of matrix-supported gravels, unsorted massive gravels and cross-bedded gravels (facies Gcm, Gpt; Fig. 7c2). Clasts of the gravels are sub-rounded to sub-angular and the matrix is composed of medium to coarse sand. Intercalations of many levels of gravel and sand, with lenticular shapes and erosional bases are frequent. Desiccation cracks developed on silt (facies Fm) and layers with chemical precipitation (facies P) are also observed, which suggests abandoned channels and periods of stability. The common development of cross

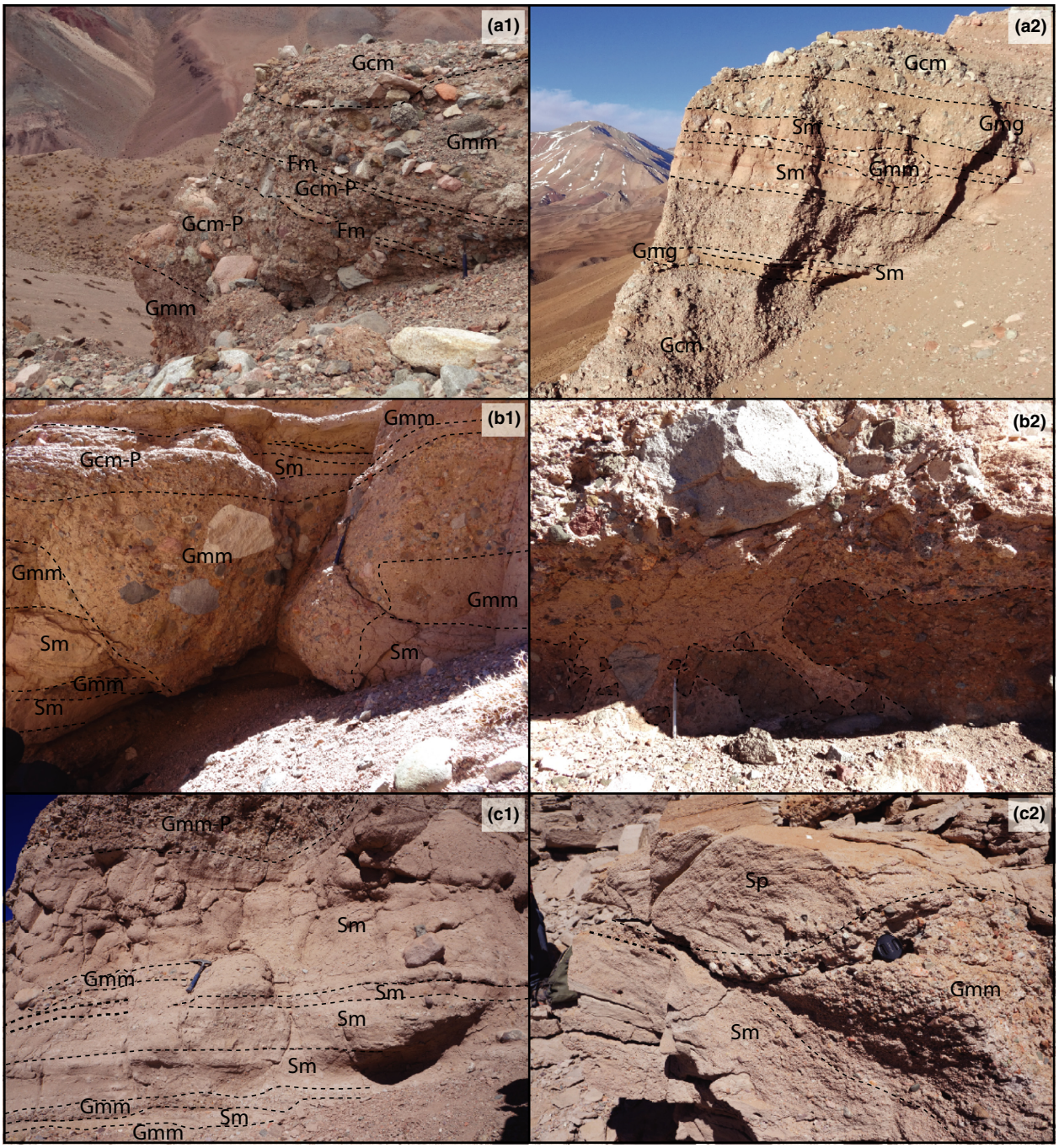

Fig. 7. Outcrop photographs of the stratigraphic sequences. The names of the lithofacies are adapted from Miall (1996), and described in Table 1. (a1) lithofacies association of the base of the Laguna Grande Succession (Column A), represented by thick clast-supported gravels; (a2) lithofacies association of the top of the Laguna Grande Succession (Column A), characterized by a greater content of matrix-supported gravels and sands; (b1) lithofacies association observed to the east of Column A, mainly composed by matrix-supported gravels and sand layers (Column B); (b2) brownish less dense and disaggregated load casts only observed in Column B; (c1 and c2) lithofacies association of the Quebrada Larga Succession, where predominant sandy facies are observed.

lamination and stratification indicates the dominance of turbulent flows, as well as the abundance of gullies carved in older deposits. This suggests a sheet flood dominated alluvial fan environment (Blair & McPherson, 1994).

The Quebrada Larga Succession is composed predominantly by fine sediments, which were deposited as diluted flows with channel infill (lens shaped bodies), and minor occurrences of matrix-supported debris flows (Fig. 8), which differs from the facies identified in the Laguna Grande Succession.

Sand composition and sedimentary provenance

In general, the gravels are composed of granitic, granodioritic, dioritic and extrusive fragments. Granitic clasts

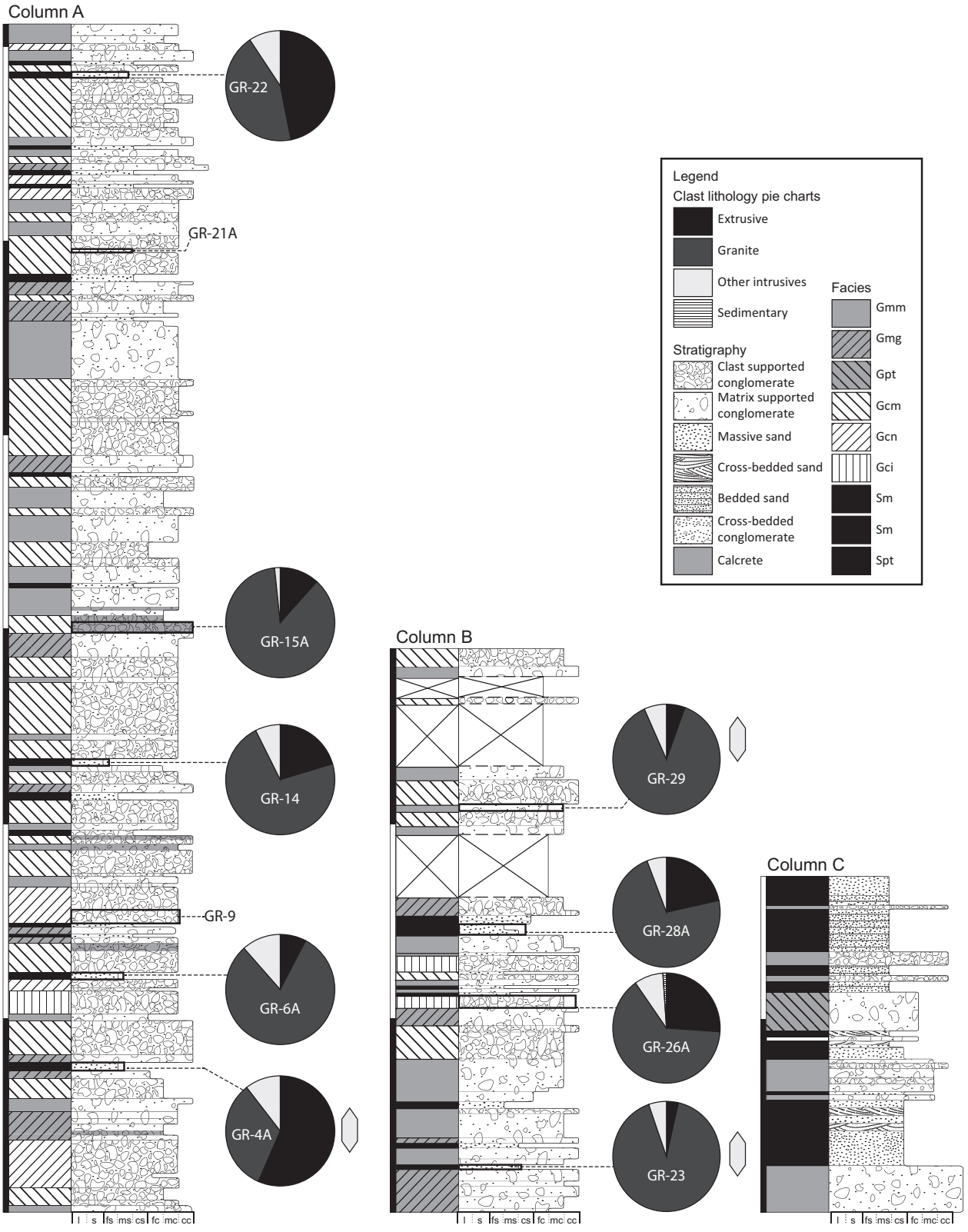

Fig. 8. Code of facies association (see Table 1 for description and depositional environment interpretation), stratigraphic column, and pie charts which indicate the amounts of most abundant clasts of columns A, B and C. Diamonds represent the samples where detrital zircon ages have been determined. Every bar in the vertical scale represents 50 m.

include monzogranite and syenogranite, both with middle to coarse grain. Monzogranite presents biotite and scarce amphibole, and a pinkish characteristic colour, whereas the syenogranite present muscovite and amphibole, and a reddish colour. Middle grain granodiorite fragments present amphibole and biotite, and a white-greyish colour.

Dioritic fragments have a fine to middle grain, and a greyish appearance. On the other hand, volcanic clasts include effusive and tuff fragments. In general, they correspond to andesites, with minor content of dacites and basalts. The tuffs are crystalline and have a greyish colour.

In general, in the western column of the Laguna Grande Succession, the most abundant gravel fragments are the granites, followed by lavas, granodiorites and diorites and tuffs. To the east, this proportion is maintained, although in some cases the lava fragments exceed the granitic clasts.

Samples of sands of the Laguna Grande Succession are composed by variable amounts of lithic fragments (2–20%), quartz (20–50%) and feldspar (40–65%). Obtained data were plotted on the provenance discrimination diagram of Dickinson *et al.* (1983). Considering only the lithic fragments, most of the samples show a predominance of intrusive grains, followed by volcanic grains and scarce sedimentary grains (Fig. 8). In some cases volcanic content is intermediate (samples GR-14, 26A and 28A). The basal and top samples of Section A (Samples GR-4A and GR-22) have more volcanic content, with minor plutonic contributions, indicating an arc signature (Fig. 9). In contrast, the rest of the samples show an uplifted basement signature (Fig. 9).

Volcanic rocks outcrop in all morphostructural systems surrounding the CBG. Some of them are partly intruded by Permo-Triassic granitic plutons (Laguna Chica and Guanaco Sonso Formations), while others are unconformably overlying them (La Totora Formation, El Gaucho Beds and Escabroso Formation). Therefore, the relative abundance on volcanic fragments on the top sample may be explained by the unroofing of any of the basement blocks or simply by the growth of the drainage network by regressive erosion through a heterogeneous bedrock. On the other hand, the basal volcanic rich sample could proceed from the erosive surface carved in the Eocene El Gaucho Beds, northwest of the CBG, or from the early Miocene volcanic succession located below the gravels and to the east. Sedimentary grains observed under the microscope are derived from Mesozoic series, whose outcrops are scarce and are only present in the western mountain system. Coarse grained granitic pluton is the dominant lithology around the CBG, where perthitic and myrmekitic textures are common (Salazar *et al.*, 2013; Salazar & Coloma, Accepted), determining their dominance on the grain counting analysis. Chloritized, fine-grained dioritic grains are scarce. These fragments are similar to the Eocene plutons, which outcrop mainly to the northwest of the gravels. However, these grains are not abundant, which suggests that although there was a contribution from this area, it was not significant. Finally, these results show a local provenance for the CBG, consistent with the proximal alluvial fan environment interpreted from the sedimentological analysis.

U-Pb ages of detrital zircons

We obtained 292 U-Pb age determinations of the Laguna Grande Succession: 63 were performed in a basal sample (GR-4A) from the western succession, while 110 and 119 were respectively performed in samples (GR-23 and GR-29) from the middle and top of the unit from the oriental succession (Fig. 6). Results from the morphological study of zircons through cathodoluminescence (CL) showed that most zircons have morphologies indicating an intrusive origin (Fig. 10), according to Corfu *et al.* (2003), which is consistent with grain compositions observed in thin sections (Fig. 8). Some zircons show distinctive morphological characteristics of volcanic origin, with Triassic, Eocene and Miocene ages. In addition, the Th/U ratio suggests an igneous nature for most of the analysed zircon grains, and only one zircon grain shows a Th/U ratio near the igneous-metamorphic limit (Rubatto, 2002).

The three analysed samples show very similar detrital zircon age patterns (Fig. 11). Nearly 90% of the analysed zircons in each sample are of Permo-Triassic age (Fig. 11), with a prominent main peak of Early to Middle Triassic age. However, there are differences between the three samples. The stratigraphically upper sample

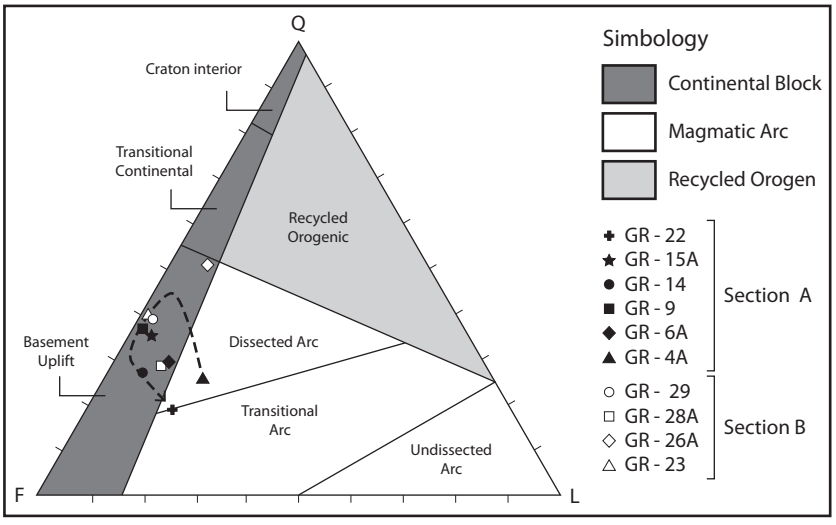

Fig. 9. QFL plot, after Dickinson *et al.* (1983), for stratigraphic columns A and B. Q = total quartz grains; F = total feldspar; and L = lithic grains.

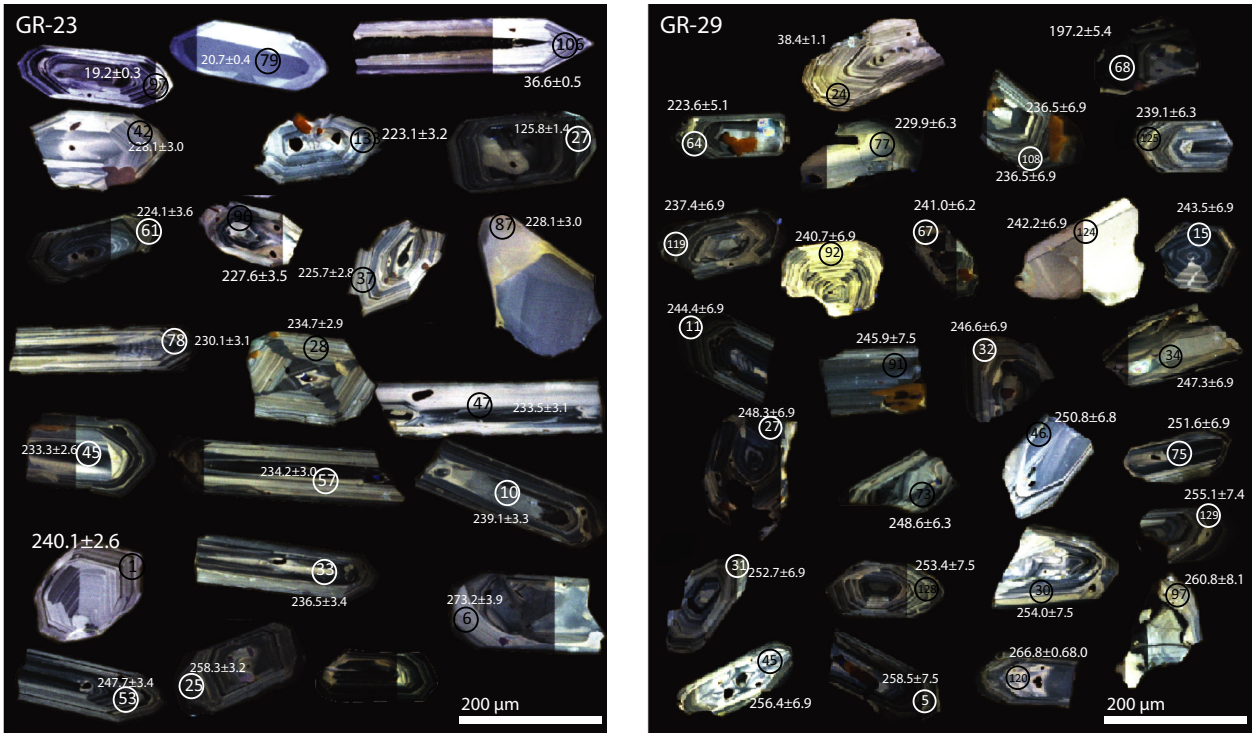

Fig. 10. Cathodoluminescence images of selected zircon grains in samples GR-23 and GR-29. The location of analysed spots and the measured ages are shown.

(GR-29) shows a peak at 246 Ma, with a dispersion tale of younger ages, while the stratigraphically lower samples (GR 23 and GR-4A) have peaks at 234 Ma and 238 Ma, respectively, with a tale dispersion of older ages. The main early to middle Triassic peak is consistent with the ages determined for the Chollay Plutonic Complex (248–237 Ma; Salazar *et al.*, 2013), the most widely exposed unit around the CBG (Fig. 2). The middle to late Permian ages may correspond to relicts of the wall rocks of the latter complex, which crop out near the Laguna Chica Lake and west of the CBG. Finally, the late Triassic zircons agree well with the age of the La Totora Formation, which unconformably overlies the Chollay Plutonic Complex.

A few Eocene zircons were identified in each sample with no statistical significance (Fig. 11). However, their systematic presence in every sample suggests a detritus supply from a source of this age. The only Eocene rocks in the area are restricted to the northwest of the CBG, corresponding to the El Gaucho Beds and the Tres Morros Plutonic Complex (Fig. 2).

The youngest zircon age population is recorded in a sample collected at the middle of the section (GR-23) with a peak at 20 Ma (Fig. 11). The basal sample GR-4A also shows two zircons with ages around 20 Ma. This data allow us to constraint the age of the CBG to a maximum of 20 Ma. Rocks of this age are those from the Escabroso Formation, which underlies the CBG and crops out in the eastern morphostructural system.

Detrital zircon and grain counting analyses indicate proximal sources for the Laguna Grande Succession of the CBG, which is consistent with the proximal alluvial fan environment inferred from the sedimentological analysis. Furthermore, the age of detrital zircons suggests sources of detritus coming mainly from the west and northwest of the CBG.

DISCUSSION

Gravels depositional environment, age and provenance

The facies observed in Laguna Grande Succession suggest a proximal alluvial fan, dominated by aggrading debris flow deposits with important coarse sediment supply in a dry environment, which grades to a more distal environment to the east and to the top. This diminution of energy with time may have occurred during the filling of the basin, due to the generalized erosion and pediplanation of the western mountain system. Sedimentation may have retrograded above a pediment surface formed by scarp retreat towards the west. Point counting in sands reveals dioritic and granodioritic fragments, which agrees with the identified facies. These fragments, indeed, are indicative of a contribution from the west and northwest, where pediments are described by the geomorphologic analysis (Las Pintadas low relief Surface; Figs 5 and 6). The youngest age in the detrital zircon is 19 Ma, indicating the maximum possible age of the Laguna Grande Succession. These Miocene ages correspond to the volcanic Escabroso Formation. This formation outcrops to the east of the gravel deposits, in the mountain system uplifted by

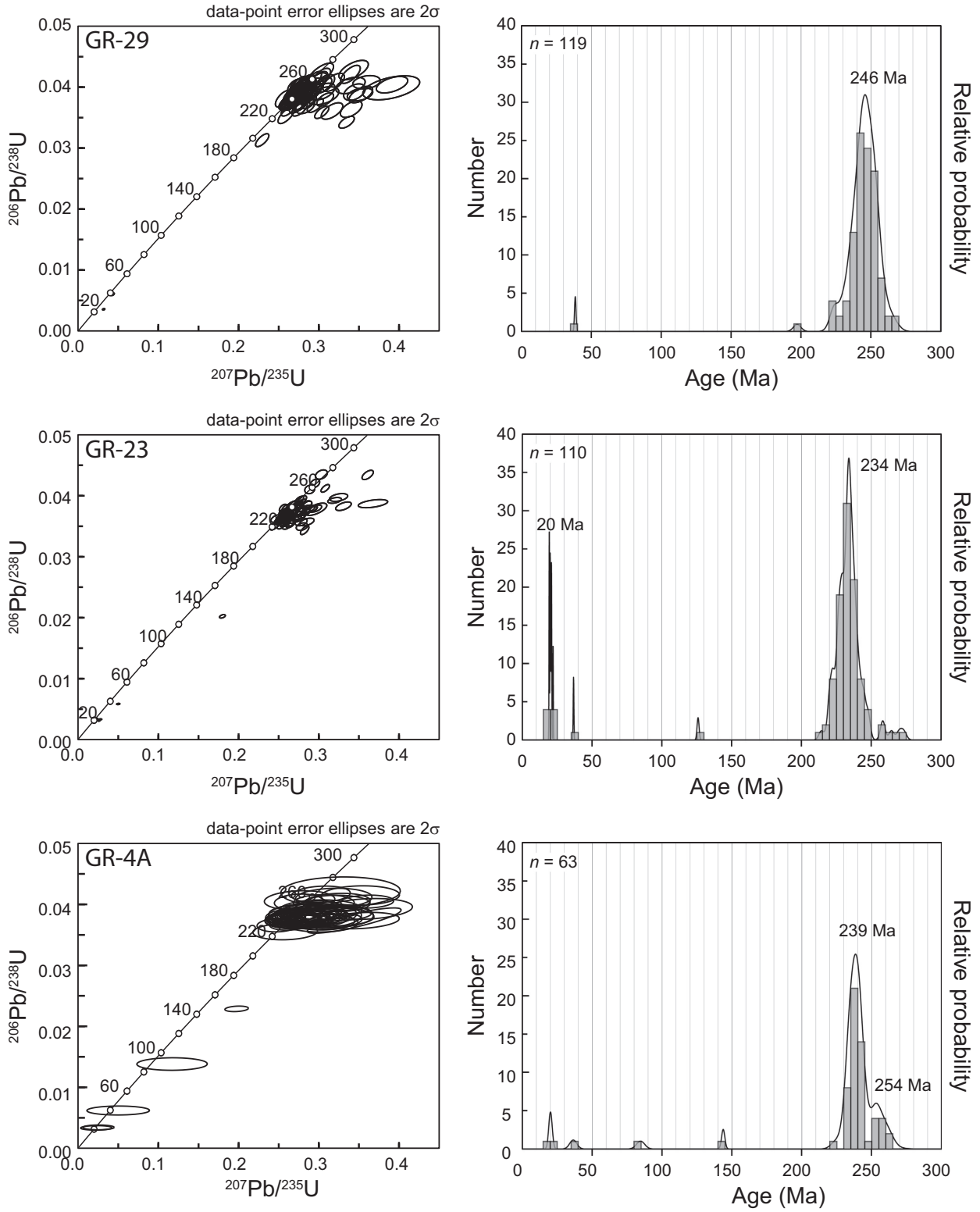

Fig. 11. Concordia diagrams and probability diagrams of detrital zircons ages for different samples.

the La Coipa-El Potro Fault System, and is partially covered by gravels.

The clast composition of the Quebrada Larga Succession is similar to that observed in the Laguna Grande Succession, although is composed predominantly by fine grain sediments deposited as diluted flows. This succession resulted from a sheet flood dominated alluvial fan environment, suggesting a development due to the remobilization and redeposition of the Laguna Grande Succession, instead of a common provenance. The Quebrada Larga Succession is located in a lower elevation compared to the Laguna Grande Succession, because it

formed following the incision and rework of this unit. The 13 Ma-old dacitic tuff intercalated in gravels of the Quebrada Larga Succession, in addition to geomorphological and stratigraphic observations, indicates an erosional discordance between these successions, and confirms that the Quebrada Larga Succession deposited after the Laguna Grande Succession. According to the youngest age in the detrital zircons and the age of the dacitic tuff the deposition of the Laguna Grande Succession occurred between 19 and 13 Ma, implying that the incision and reworking started close to 13 Ma.

Mountain building and landscape evolution

Many studies in Northern Chile, Southern Perú and Bolivia, have shown that the Central Andes have grown during the Cenozoic in response to crustal shortening and thickening processes (Isacks, 1988; Garzione *et al.*, 2008; Strecker *et al.*, 2009).

In the following sections we analyse the morphostratigraphic and tectonic evolution of the studied area (Fig. 12), constrain the timing of mountain building, the landscape evolution resulting from the erosive response, and compare with other studies in neighbouring regions (Fig. 13).

Eocene–Oligocene orogenesis and pedimentation

The evolution of the studied area is largely controlled by the uplift of the western mountain system above the Valeriano Fault (Fig. 12a). Geological observations indicate that the activity of this fault is bracketed between 63 and 21 Ma, i.e. before the deposition of the Laguna Grande Succession (Fig. 3a). However, three main geological observations indicate a fault activity largely older than the early Miocene: (1) the presence of the Las Pintadas Surface, which is carved on the western system, (2) the current absence of a topographic expression of the fault itself, and (3) the Eocene El Gaucho beds unconformably overlying the basement and Mesozoic units in the hanging wall (Fig. 3). This interpretation agrees with the internal syncline affecting a 46 Ma tuff sealed by a 44 Ma tuff observed in the northern basement system (Fig. 3b), which corresponds to the most recent activity that affected the western mountain system. Thus, the main activity of the Valeriano Fault most likely occurred between 63 and 45 Ma (Fig. 13), and we can constrain the uplift of this mountain system before ~45 Ma.

Sixty kilometre west of the studied area, geological observations of Pineda & Emparán (2006), Creixell *et al.* (2013) and Salazar *et al.* (2013), based on contact relationships and chronological analyses, evidence a late Eocene activity on a ~150 km-long thrust system (Vicuña and Rivadavia faults) with both west and east vergences. Around 110 km to the south, in the El Indio Belt (~30°S), Martin *et al.* (1997) described a structural domain in which north-striking, high-angle, reverse faults were active between 54 and 27 Ma, which could be related to

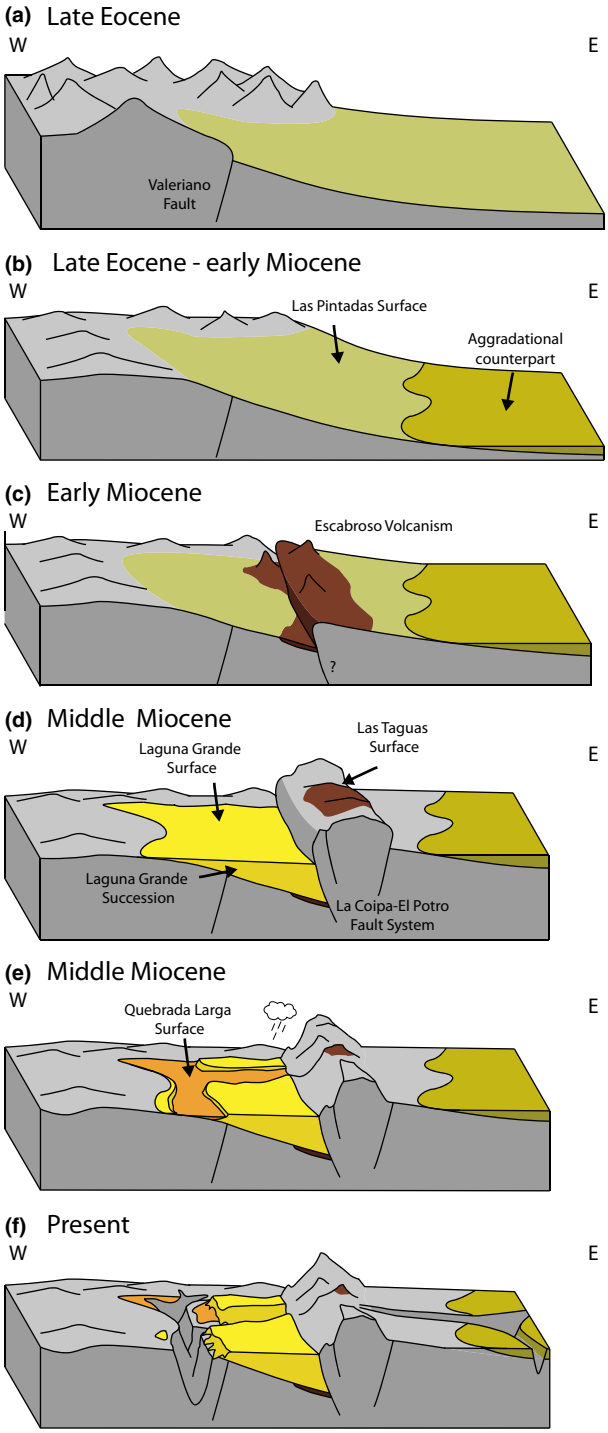

Fig. 12. Evolution of studied area from Eocene to present. (a) Late Eocene: the "Incaic Relief" dominates the geography in the west and northwest areas; (b) pedimentation processes following the "Incaic" orogeny; (c) volcanism developed during early Miocene; (d) accumulation of the Laguna Grande Succession; (e) hydrological reconfiguration, due to the establishment of a climatic barrier, leading to the Quebrada Larga Succession development; (f) major effects of hydrological reconfiguration with the development of the Los Tambillos gravels and the final modern valley incision.

the Eocene deformation described in the studied area. Recent studies developed near 28°S identify a compressive pulse during the early Paleocene, based on an angular

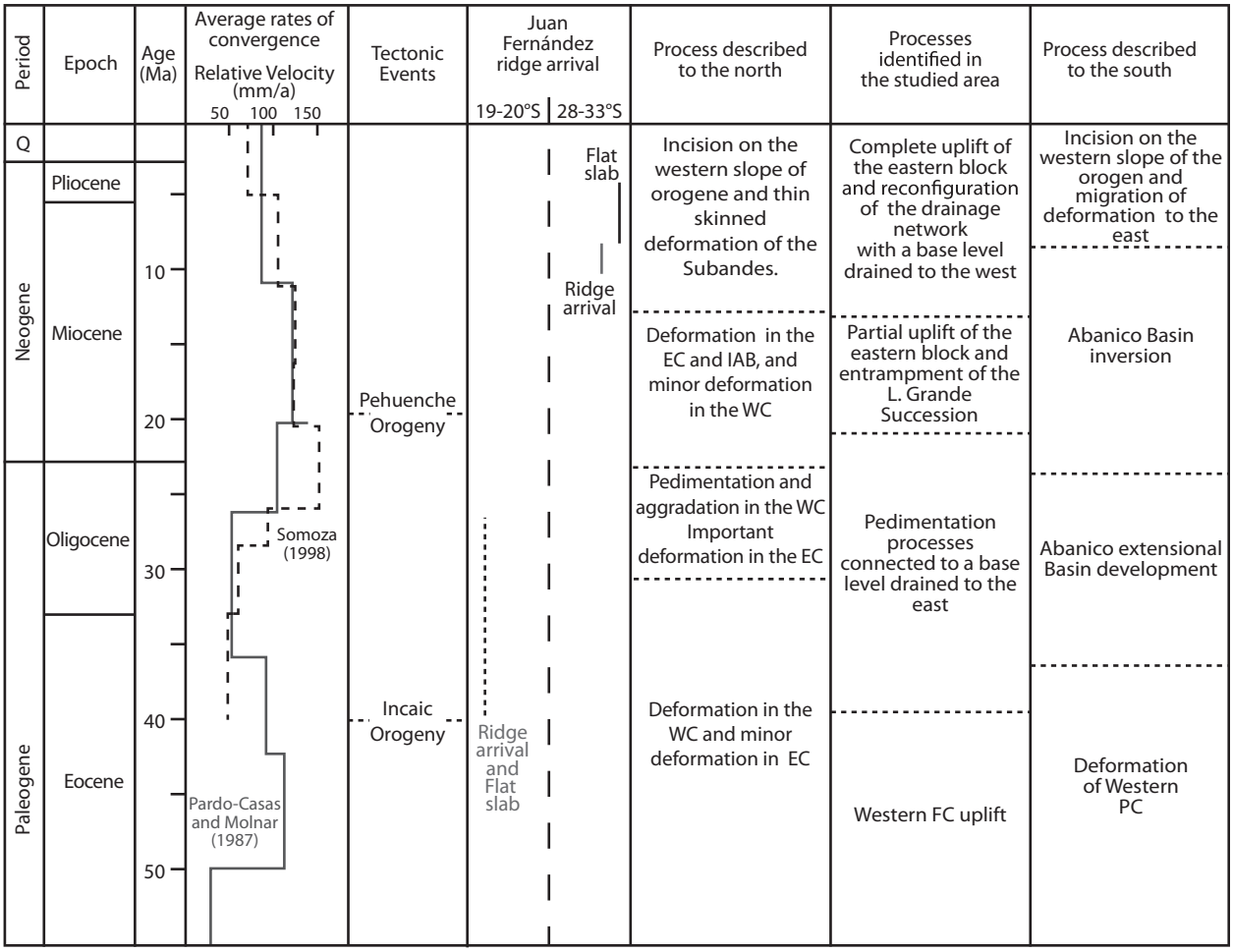

Fig. 13. Summary of major tectonic processes identified in the studied area and described for the regions further north and south. Average rates of convergences are included, according to Pardo-Casas & Molnar (1987) and Somoza (1998). We indicate the average ages of tectonic phases acknowledging that they vary latitudinally.

unconformity between the synorogenic Quebrada Seca Formation (65–60 Ma) and the late Jurassic Lagunillas Formation (Martínez *et al.*, 2015). All these studies indicate that the deformation of the western Frontal Cordillera was accommodated by several thrust systems during the Paleogene.

Recent reconstructions developed further north (~20°S) reveal that the main shortening and crustal thickening processes occurred between 50 and 30 Ma (Fig. 13; Maksaev & Zentilli, 1999; Armijo *et al.*, 2015), under a thick-skinned structural style (Muñoz & Charrier, 1996). This episode of compressive deformation corresponds to the "Incaic phase" (e.g., Steinman, 1929; Noble *et al.*, 1990; Charrier *et al.*, 2007, 2009), and it resulted in the uplift of the Western Cordillera, the Domeyko Range and the Frontal Cordillera. The faults geometry and kinematics in the Western Cordillera indicate that the uplift of the relief was accommodated by bivergent thrusts (Maksaev & Zentilli, 1999; Charrier *et al.*, 2007, 2009). Mountain systems uplifted during this period correspond to a continuous 60–100 km wide NNE oriented belt that extends from southern Perú to central Chile (Charrier *et al.*, 2009). Eocene shortening also occurred in the Central and Eastern Altiplano, and in the Eastern Cordillera, although with minor shortening rates (Elger *et al.*, 2005; Oncken *et al.*, 2006).

After the Middle Eocene the deformation decreased in the Western Cordillera (McQuarrie *et al.*, 2005; Lamb *et al.*, 1997). The landscape of the Western Cordillera and Domeyko Range was characterized by more stable conditions, evidenced by the development of a pediplain in the western slope of the range (Segerstrom, 1963; Galli-Olivier, 1967; Sillitoe *et al.*, 1968; Mortimer, 1973), and by the aggradation of gravels derived from the erosion of the Eocene range. The latter, in turn, were deposited in the western (e.g., Nalpas *et al.*, 2008; : Riquelme *et al.*, 2007) and in the eastern slope (Charrier *et al.*, 2009) of the Eocene relief. On the other hand, further south (32–36°S) there is no record of Eocene compressive deformation. In addition, there is evidence of the development of the Abanico Basin in an extensional setting during 36 Ma and late Oligocene-early Miocene (Charrier *et al.*, 2007, 2009; Rodríguez, 2013; Jara & Charrier, 2014; Winocur *et al.*, 2014).

Our observations suggest a similar pedimentation context during the Eocene-Oligocene in the studied area.

Indeed, the landscape was characterized by more stable conditions after the Eocene uplift of the western mountain system. These conditions allowed the development of the Las Pintadas Surface between 44 and 21 Ma. It suggests that the base level did not drop significantly (e.g., Burbank & Anderson, 2001; Dohrenwend & Parsons, 2009) during the Eocene-Oligocene. 100 km to the south, in the El Indio Belt (~30°S) pedimentation processes have also been registered in Argentina and Chile (Bissig *et al.*, 2002; Aguilar *et al.*, 2011). At this latitude some continental successions were identified to the east, in the Valle del Cura in Argentina, deposited during Eocene and early Oligocene (Limarino *et al.*, 1999). This deposit could correspond to the aggradational counterpart of the pedimentation of the Eocene relief in this region (Fig. 12b).

Miocene migration of deformation and intramontane basin configuration

Similar to other regional studies (Reutter, 1974; Nalpas *et al.*, 2009; Moscoso *et al.*, 2010) our field observations indicate that the CBG deposits are cut by the La Coipa-El Potro fault System (Figs 2, 4b and 6). The uplift of the eastern mountain system represented a topographic barrier that triggered the blocking of sediment transport, resulting in the establishment of an intramontane depocenter, and giving way to the deposition of the Laguna Grande Succession between 19 and 13 Ma (Fig. 12d). This hypothesis is supported by several observations. On the one hand, the Laguna Grande Succession shows detrital zircon data that records Miocene ages. It contains more subangulous fragments next to the trace of La Coipa-El Potro Fault System, and shows evidence of deformation. On the other hand, the Las Taguas Surface, which corresponds to the eastern continuation of the Las Pintadas Surface, shows a lack of a gravel cover.

Evidences of early-middle Miocene compressive pulse have also been documented in the Chilean Frontal Cordillera, immediately to the north and south of the studied zone. Near 28°S an early Miocene compressive pulse is evidenced by an angular unconformity between the Quebrada Seca Formation and the Doña Ana Group, which also shows deformation and faulting during this period of time (Martínez *et al.*, 2015). Around 29°S, Martin *et al.* (1997) described structures cutting and folding The Escabroso Formation that are covered by 16 Ma units, which indicates that a deformation event occurred between 18 and 16 Ma. Thermal modelling data registered to the south, in the Elqui and Limarí Valleys (30–31°S) also suggest an early-middle Miocene compressive pulse inverting an Oligocene extensional intra-arc basin (Rodríguez, 2013).

Similar to the Chilean Frontal Cordillera, there are evidences of deformation during late Oligocene and late Miocene, which contributed to the growth of the central Andes in other physiographic units (Fig. 13). Further north (~20°S) evidence of crustal shortening and thickening has been documented in the whole Central Andes since the Eocene (Elger *et al.*, 2005; Oncken *et al.*, 2006). However, during the Miocene, deformation was focalized to the east, in the Eastern Cordillera and Altiplano (Sempere *et al.*, 1990; Lamb *et al.*, 1997; Gregory-Wodzicki, 2000; McQuarrie *et al.*, 2005; Armijo *et al.*, 2015). Further south (32–36°S) a regional compressive event resulted in the partial inversion of the Abanico Basin, during late Oligocene and late Miocene (Charrier *et al.*, 2002, 2007, 2009; Farías *et al.*, 2010; Jara & Charrier, 2014; Muñoz-Sáez *et al.*, 2014). Miocene inversion is marked by the progressive migration of shortening from the boundaries of the former Abanico Basin in the early Miocene, to the eastern parts of the range following 16 Ma (Farías *et al.*, 2010). Based on the previous description, Miocene compression and migration to the east, would be a generalized evolution in the Central Andes, involving different physiographic units, transcending diverse morphotectonic conditions.

Hydrological reconfiguration and valley incision during late Miocene and Plio-Quaternary

We propose that the Laguna Grande succession resulted from the aggradation of sediments in an intramontane basin (Fig. 12d). Later, the Laguna Grande Surface was abandoned and incised, evidencing a drop in the base level. Gravels were eroded and the contact surface between bedrock and gravels (Las Pintadas Surface) was exhumed and covered again by the Quebrada Larga Succession. Considering the textural characteristic of its sediments and the location of deposit, we argue that this incision was connected to a base level that drained to the west (Fig. 12e). Therefore, the construction of the Quebrada Larga Surface marks the beginning of a hydrological reconfiguration. The tuff intercalated in the base of the Quebrada Larga Succession suggests that this reconfiguration began after 13 Ma. It may be a consequence of the middle Miocene uplift of the eastern mountain system, produced by the activity of La Coipa-El Potro Fault System. Afterwards, bedrock incision developed the current configuration of valleys (Fig. 12f).

At 28–30°S, erosion of low relief surfaces indicates an incision event during the late Miocene and Pliocene in the whole forearc, as evidenced by the Quebrada Larga Surface in the studied area, the Los Ríos Surface in the El Indio Belt (Bissig *et al.*, 2002), the Corredores Surface in the Domeyko Basin (Rodríguez *et al.*, 2014) and the Vallenar Terraces in the Huasco Valley (Mortimer, 1973). Similarly, valley incision also started during late Miocene to the north (Isacks, 1988; Lamb *et al.*, 1997; Riquelme *et al.*, 2007; Schildgen *et al.*, 2007; Farías *et al.*, 2008) and to the south of the studied area (Fig. 13; Farías *et al.*, 2008; Rodríguez *et al.*, 2014). To explain this incision event, local and regional processes have been discussed. Studies developed near 33°S suggest that the incision was influenced by the shallowing of the slab (Farías *et al.*, 2008). Although there is a temporal correspondence with the beginning of the flat subduction and the incision in the studied area, the incisional event has been described

in the complete western slope of the Central Andes, including flat and normal subduction zones (Isacks, 1988; Lamb *et al.*, 1997; Bissig *et al.*, 2002; Riquelme *et al.*, 2007; Farías *et al.*, 2008; Aguilar *et al.*, 2011), suggesting that this corresponded to a more regional event. Studies developed further north, suggest that this incisional event may have been related to the Brazilian Shield subduction (e.g., Gubbels *et al.*, 1993; McQuarrie *et al.*, 2005; Lamb, 2011) and to the uplift and westward tilting of the orogen produced by important overthrusts with vergences to the east (e.g., Isacks, 1988; Giambiagi *et al.*, 2001; Farías *et al.*, 2005; Riquelme *et al.*, 2007). The erosive response and valley incision were not necessarily coetaneous to the uplift and differential delay along the Andes can be attributed to latitudinal climatic variation and lithology of bedrock (Montgomery *et al.*, 2001).

Although most models invoke deep geodynamic processes to explain the uplift that triggered valley incision, it is also possible to explain it by the combination of geomorphological and deeper crust processes (e.g., Strecker *et al.*, 2009). The activity of La Coipa-El Potro Fault System that uplifted the eastern mountain system, like several other thrust systems along the Andes, is a factor that by itself could have widely modified the landscape evolution and triggered the westward incision. The uplift of the eastern system led to the westward catchment of the intramontane basin and the valley incision related to the increase in relief and drainage area. This has been documented in the central Andes further north (e.g., Schlunegger *et al.*, 2010) and other mountain ranges (e.g., Willet *et al.*, 2006). Complementary, the growth of the Andes increased the climatic barrier (e.g. Hain *et al.*, 2011), which concentrated the westerlies rainfall on the western slope of the orogen (Fig. 12e). It also contributed to a glacial environment developed during Quaternary, which is visible in the glacial and paraglacial geomorphology of the upstream parts of valleys (Zech *et al.*, 2006; Aguilar, 2010).

SUMMARY AND CONCLUSION

The Cerro del Burro Gravels, and preserved low relief surfaces in the Chilean Frontal Cordillera near 28°45′S provide important constraints on the Neogene erosion and denudation of the Andes. We propose the timing, magnitudes and styles of the evolution of the mountain range, which resulted in the eastward migration of the deformation and reconfiguration of the drainage network.

The evolution of the studied area can be summarized into three stages:

(1) After the middle Eocene (~44 Ma), following the uplift of the western and northern mountain systems, pedimentation processes occurred during a period of relative tectonic quiescence, which lasted until 19 Ma.
(2) Between 19 and 13 Ma the uplift of the eastern and southern mountain systems disturbed the pedimentation processes, interrupted the sediment migration to the east, and triggered the accumulation of gravels in an intramontane basin.
(3) The geological evolution of the study area is completed by the westward capture of the intramontane basin following 13 Ma, and by the current valley incision related to the increase in relief and area of basins.

ACKNOWLEDGEMENTS

This work was supported by CONICYT (Chilean National Research Agency) through the Fondecyt grant No. 11121529: Quantifying long-term denudation with low-temperature thermochronology: tectonic activity and landscape evolution of the Chilean Andes (27–32°S), by G. Aguilar and Plan Nacional de Geología from SERNAGEOMIN. We also thank the ECOS-Sud-Conicyt program (project C11U02) for financial support. This study is part of the M. Sc. thesis of K.R., in the Universidad de Chile which was supported in part by the Institut de Recherche pour le Développement (IRD, France) through the Laboratorio Mixto Internacional (LMI) COPEDIM. Authors would like to thank Dr. Andrés Folguera and two anonymous reviewers for the comments that allowed us to significantly improve our manuscript. We would like to thank M. Muñoz and B. Townley for the careful review of this manuscript.

CONFLICT OF INTEREST

No conflict of interest declared.

SUPPORTING INFORMATION

Additional Supporting Information may be found in the online version of this article:

Appendix S1. U-Pb geochronological data

Table S1. Zircon U-Pb geochronological data for sample GR-4A.

Table S2. Zircon U-Pb geochronological data for sample GR-23. Zircons shown in Fig. 10 are highlighted in bold.

Table S3. Zircon U-Pb geochronological data for sample GR-29. Zircons shown in Fig. 10 are highlighted in bold.

REFERENCES

Aguilar, G. (2010). Erosión y transporte de materia en la vertiente occidental de los Andes semiáridos del Norte de Chile (27-32° S): desde un enfoque a gran escala temporal y espacial, hasta la evolución cuaternaria de un sistema fluvial. PhD thesis, Université de Toulouse; Universidad Católica del Norte (UCN), Chile.

Aguilar, G., Riquelme, R., Martinod, J., Darrozes, J. & Maire, E. (2011) Variability in erosion rates related to the

state of landscape transience in the semi-arid Chilean Andes. *Earth Surf. Proc. Land.*, **36**, 1736–1748.

Allmendinger, R., Ramos, V., Jordan, T., Palma, M. & Isacks, B. (1983) Paleogeography and Andean structural geometry, northwest Argentina. *Tectonics*, **2**, 1–16.

Armijo, R., Lacassin, R., Coudurier-Curveur, A. & Carrizo, D. (2015) Coupled tectonic evolution of Andean orogeny and global climate. *Earth Sci. Rev.*, **143**, 1–35.

Ballato, P., Cifelli, F., Heidarzadeh, G., Ghassemi, M.R., Wickert, A.D., Hassanzadeh, J., Dupont-Nivet, G., Balling, P., Sudo, M., Zeilinger, G., Schmitt, A.K., Mattei, M. & Strecker, M.R. (2016) Tectono-sedimentary evolution of the northern Iranian Plateau: insights from middle-late Miocene foreland-basin deposits. *Basin Res.*, **12180**, 1–30.

Barazangi, M. & Isacks, B. (1976) Spatial distribution of earthquakes and subduction of the Nazca plate beneath South America. *Geology*, **4**, 686–692.

Bissig, T., Clark, A. & Lee, J. (2002) Miocene landscape evolution and geomorphologic controls on epithermal processes in the El Indio-Pascua Au-Ag-Cu Belt, Chile and Argentina. *Econ. Geol.*, **97**, 971–996.

Blair, T. & McPherson, J. (1994) Alluvial fans and their natural distinction from rivers. *J. Sediment. Res.*, **64**, 450–489.

Blair, T. & McPherson, J. (1999) Grain size and textural classification of coarse sedimentary particles. *J. Sediment. Res.*, **69**, 6–19.

Burbank, D. & Anderson, R. (2001) *Tectonic Geomorphology*. Blackwell Science, Oxford.

Cahill, T. & Isacks, B. (1992) Seismicity and Shape of the Subducted Nazca Plate. *J. Geophys. Res.*, **97**, 17503–17529.

Charrier, R., Alvarez, P. & Zurita, E. (2002) Evidence for Cenozoic extensional basin development and tectonic inversion south of the flat-slab segment, southern Central Andes, Chile (33°-36° S.L). *J. S. Am. Earth Sci.*, **15**, 117–139.

Charrier, R., Pinto, L. & Rodríguez, M.P. (2007) Tectonostratigraphic evolution of the Andean Origen in Chile. In: *The Geology of Chile* (Ed. by T. Moreno, W. Gibbons), pp. 21–114. The Geological Society, London.

Charrier, R., Farías, M. & Maksaev, V. (2009) Evolución tectónica, paleogeográfica y metalogénica durante el Cenozoico en los Andes de Chile Norte y Central e implicaciones para las regiones adyacentes de Bolivia y Argentina. *Rev. Asoc. Geol. Argentina*, **65**, 5–35.

Coira, B., Davidson, C., Mpodozis, C. & Ramos, V. (1982) Tectonic and magmatic evolution of the Andes of northern Argentina and Chile. *Earth Sci. Rev.*, **18**, 303–332.

Contreras, J. & Schilling, M. (2012). Geología del área San Fernando-Curicó. Servicio Nacional de Geología y Minería. Carta geológica de Chile, Serie Geología Básica. 1 mapa escala 1:100.000.

Corfu, F., Hanchar, J., Hoskin, P. & Kinny, P. (2003) Atlas of Zircon Textures. In: *Zircon. Mineralogical Society of America, Reviews in Mineralogy and Geochemistry 53* (Ed. by J. Hanchar, P. Hoskin), pp. 469–500. Mineralogical Society of America, Washington, DC, USA.

Creixell, C., Labbé, M., Arévalo, C. & Salazar, E. (2013). Geología del área Estación Chañar-Junta de Chingoles. Regiones de Atacama y Coquimbo. Servicio Nacional de Geología y Minería. Carta geológica de Chile, Serie Geología Básica 150. 1 mapa escala 1:100.000.

DeCelles, P., Gray, M., Ridgway, K., Cole, R., Pivnik, D., Pequera, N. & Srivastava, P. (1991) Controls on synorogenic alluvial-fan architecture, Beartooth Conglomerate (Palaeocene), Wyoming and Montana. *Sedimentology*, **38**, 567–590.

Dickinson, W. (1970) Interpreting detrital modes of graywacke and arkose. *J. Sediment. Petrol.*, **40**, 695–707.

Dickinson, W.R., Beard, L.S., Brakenridge, G.R., Erjavec, J.L., Ferguson, R.C., Inman, K.F., Knepp, R.A., Lindberg, F.A. & Ryberg, P.T. (1983) Provenance of North American Phanerozoic sandstones in relation to tectonic setting. *Geol. Soc. Am. Bull.*, **94**, 222–235.

Dohrenwend, J. & Parsons, A. (2009) Pediments in Arid Environments. In: *Geomorphology of Desert Environments*. 2nd edn (Ed. by A. Parsons, A. Abrahams), pp. 377–411. Chapman and Hall, Springer, London.

Elger, K., Oncken, O. & Glodny, J. (2005) Plateau-style accumulation of deformation: Southern Altiplano. *Tectonics*, **24**, TC4020.

Espurt, N., Funiciello, F., Martinod, J., Guillaume, B., Regard, V., Faccena, C. & Brusset, S. (2008) Flat subduction dynamics and deformation of the South American plate: Insights from analog modeling. *Tectonics*, **27**, TC3011.

Farías, M., Charrier, R., Comte, D. & Martinod, J. (2005) Late Cenozoic deformation and uplift of the western flank of the Altiplano: Evidence from the depositional, tectonic, and geomorphologic evolution and shallow seismic activity (northern Chile at 19°30′S). *Tectonics*, **24**, TC4001.

Farías, M., Charrier, R., Carretier, S., Martinod, J., Fock, A., Campbell, D., Cáceres, J. & Comte, D. (2008) Late Miocene high and rapid surface uplift and its erosional response in the Andes of Central Chile (33°-35°S). *Tectonics*, **27**, TC1005.

Farías, M., Comte, D., Charrier, R., Martinod, J., David, C., Tassara, A., Tapia, F. & Fock, A. (2010) Crustal-scale structural architecture in central Chile based on seismicity and surface geology: Implications for Andean mountain building. *Tectonics*, **29**, TC3006.

Galli-Olivier, C. (1967) Pediplain in Northern Chile and the Andean Uplift. *Science*, **158**, 653–655.

Garzione, C.N., Hoke, G.D., Libarkin, J.C., Withers, S., MacFadden, B., Eiler, J., Ghosh, P. & Mulch, A. (2008) Rise of the Andes. *Science*, **320**, 1304–1307.

Gazzi, P. (1966) Le arenarie del flysch sopracretaceo dell'Appennino modenese; correlazioni con il flysch di Monghidoro. *Miner. Petrogr. Acta*, **12**, 69–97.

Gehrels, G. (2009) *Age Pick Program*. University of Arizona Laserchron Center, USA.

Giambiagi, L., Tunik, M. & Ghiglione, M. (2001) Cenozoic tectonic evolution of the Alto Tunuyán foreland basin above the transition zone between the flat and normal subduction segment (33°30′-34°S), western Argentina. *J. S. Am. Earth Sci.*, **14**, 707–724.

Gregory-Wodzicki, K.M. (2000) Uplift history of the Central and Northern Andes: A Review. *Geol. Soc. Am. Bull.*, **112**, 1091–1105.

Gubbels, T., Isacks, B. & Farrar, E. (1993) High-level surfaces, plateau uplift, and foreland development, Bolivian central Andes. *Geology*, **21**, 695–698.

Gutscher, M.-A., Spakman, W., Bijwaard, H. & Engdahl, E. (2000) Geodynamics of flat subduction: Seismicity and tomographic constraints from the Andean margin. *Tectonics*, **19**, 814–833.

Hain, M., Strecker, M., Bookhagen, B., Alonso, R., Pingel, H. & Schmitt, A. (2011) Neogene to Quaternary broken

foreland formation and sedimentation dynamics in the Andes of NW Argentina (25°S). *Tectonics*, **30**, TC2006.

Horton, B. & Schmitt, J. (1996) Sedimentology of the lacustrine fan-delta system, Miocene Horse Camp Formation, Nevada, USA. *Sedimentology*, **43**, 133–155.

Ingersoll, R., Bullard, T., Ford, R., Grimm, J., Pickle, J. & Sares, S. (1984) The effect of grain size on detrital modes: A test of the Gazzi - Dickinson point - counting method. *J. Sediment. Petrol.*, **54**, 0103–0116.

Isacks, B. (1988) Uplift of the Central Andes plateau and bending of the Bolivian Orocline. *J. Geophys. Res.*, **93**, 3211–3231.

Jaillard, E. & Soler, P. (1996) Cretaceous to early Paleogene tectonic evolution of the northern Central Andes (0-18°S) and its relations to geodynamics. *Tectonophysics*, **259**, 41–53.

Jara, P. & Charrier, R. (2014) Nuevos antecedentes estratigráficos y geocronológicos para el Meso-Cenozoico de la Cordillera Principal de Chile entre 32° y 32°30′S: Implicancias estructurales y paleogeográficas. *Andean Geol.*, **41**, 174–209.

Jordan, T., Isacks, B., Allmendinger, R., Brewer, J., Ramos, V. & Ando, C. (1983) Andean tectonics related to geometry of subducted Nazca plate. *Geol. Study Am. Bull.*, **94**, 341–361.

Kay, S. & Mpodozis, C. (2002) Magmatism as a probe to the Neogene shallowing of the Nazca plate beneath the modern Chilean flat-slab. *J. S. Am. Earth Sci.*, **15**, 29–57.

Kay, S., Maksaev, V., Moscoso, R., Mpodozis, C., Nasi, C. & Gordillo, C. (1988) Tertiary Andean magmatism in Chile and Argentina between 28°S and 33°S: Correlation of magmatic chemistry with a changing Benioff zone. *J. S. Am. Earth Sci.*, **1**, 21–38.

Lamb, S. (2011) Did shortening in thick crust cause rapid Late Cenozoic uplift in the northern Bolivian Andes? *J. Geol. Soc. London*, **168**, 1079–1092.

Lamb, S., Hoke, L., Kennan, L. & Dewey, J. (1997) Cenozoic evolution of the Central Andes in Bolivia and northern Chile. *Geol. Soc. Spec. Pub.*, **121**, 237–264.

Limarino, C., Gutiérrez, P., Malizia, D., Barreda, V., Page, S., Ostera, H. & Linares, E. (1999) Edad de las secuencias paleógenas y neógenas de las cordilleras de la Brea y Zancarrón, Valle del Cura, San Juan. *Rev. Asoc. Geol. Argentina*, **54**, 177–181.

Ludwig, K. (2003). *Isoplot 3.0. A Geochronological Toolkit for Microsoft Excel*. Special publication n° 4. Berkeley Geochronology Center, Berkeley, California.

Maksaev, V. & Zentilli, M. (1999) Fission track thermochronology of the Domeyko Cordillera, northern Chile: implications for Andean tectonics and porphyry copper metallogenesis. *Explor. Min. Geol.*, **8**, 65–89.

Martin, M., Clavero, J. & Mpodozis, C. (1997) Eocene to Late Miocene structural development of Chile's El Indio gold belt, 30°S.*VIII Congreso Geológico Chileno. Antofagasta*, **1**, 144–148.

Martínez, F., Arriagada, C., Valdivia, R., Deckart, K. & Peña, M. (2015) Geometry and kinematics of the Andean thick-skinned thrust systems: Insights from the Chilean Frontal Cordillera (28°-28.5°S), Central Andes. *J. S. Am. Earth Sci.*, **64**, 307–324.

Martínez, F., Arriagada, C., Peña, M., Deckart, K. & Charrier, R. (2016) Tectonic styles and crustal shortening of the Central Andes "Pampean" flat-slab segment in northern Chile (27–29°S). *Tectonophysics*, **667**, 144–162.

Martinod, J., Husson, L., Roperch, P., Guillaume, B. & Espurt, N. (2010) Horizontal subduction zones, convergence velocity and the building of the Andes. *Earth Planet. Sci. Lett.*, **299**, 299–309.

Martinod, J., Guillaume, B., Espurt, N., Faccena, C., Funiciello, F. & Regard, V. (2013) Effect of aseismic ridge subduction on slab geometry and overriding plate deformation: Insights from analogue modeling. *Tectonophysics*, **588**, 39–55.

McQuarrie, N., Horton, B.K., Zandt, G., Beck, S. & DeCelles, P.G. (2005) Lithospheric evolution of the Andean fold-thrust belt, Bolivia, and the origin of the central Andean plateau. *Tectonophysics*, **399**, 15–37.

Miall, A. (1996) *The Geology of Fluvial Deposits - Sedimentary Facies, Basin*. Springer, Berlín.

Montgomery, D., Balco, G. & Willet, S. (2001) Climate, tectonics, and the morphology of the Andes. *Geology*, **29**, 579–582.

Mora, C. (2014) *Geología Estructural y Arquitectura Estratigráfica de la Cuenca Jurásico Superior de Lagunillas, Alta Cordillera de Vallenar*. Departamento de Ciencias de la Tierra, Universidad de Concepción, Chile, Región de Atacama. Memoria para optar al título de Geólogo.

Mortimer, C. (1973) The Cenozoic history of the southern Atacama Desert, Chile. *J. Geol. Soc.*, **129**, 505–526.

Moscoso, R., Mpodozis, C., Nasi, C., Ribba, L. & Arévalo, C. (2010). Geología de la Hoja El Tránsito, Región de Atacama. Servicio Nacional de Geología y Minería. Carta geológica de Chile. Serie Preliminar 7. 1 mapa escala 1:250.000, 3 anexos. Santiago.

Mpodozis, C. & Gardeweg, M. (2008). Updated Regional Geology of El Morro District (1:25.000 scale). Aurum Consultores, internal report for XStrata Copper, Santiago.

Muñoz, N. & Charrier, R. (1996) Uplift of the western border of the Altiplano on a west-vergent thrust system, Northern Chile. *J. S. Am. Earth Sci.*, **9**, 171–181.

Muñoz-Sáez, C., Pinto, L., Charrier, R. & Nalpas, T. (2014) Influence of depositional load on the development of a short-cut fault system during the inversion of an extensional basin: The Eocene-Oligocene Abanico Basin case, central Chile Andes (33°-35°S). *Andean Geol.*, **41**, 1–28.

Nalpas, T., Dabard, M.-P., Ruffet, G., Vernon, A., Mpodozis, C., Loi, A. & Hérail, G. (2008) Sedimentation and preservation of the Miocene Atacama Gravels in the Pedernales-Chañaral Area, Northern Chile: Climatic or tectonic control? *Tectonophysics*, **459**, 161–173.

Nalpas, T., Dabard, M., Pinto, L. & Loi, A. (2009). Preservation of the Miocene Atacama Gravels in Vallenar area, northern Chilean Andes: Climate, stratigraphic or tectonic control? XII Congreso Geológico Chileno, Santiago, S9_063.

Noble, D., McKee, E., Mourier, T. & Mégard, F. (1990) Cenozoic stratigraphy, magmatic activity, compressive deformation, and uplift in northern Peru. *Geol. Soc. Am. Bull.*, **102**, 1105–1113.

Oncken, O., Hindle, D., Kley, J., Elger, K., Víctor, P. & Schemmann, K. (2006) Deformation of the Central Andean Upper Plate System – Facts, Fiction, and Constraints for Plateau Models. In: *The Andes - Active Subduction Orogeny* (Ed. by O. Oncken, G. Chong, G. Franz, P. Giese, H.-J. Götze, V. Ramos, M.R. Strecker, P. Wigger), pp. 3–28. Springer, Berlin.

Ortiz, M. & Merino, R. (2015). Geología del área río Chollay-Matancilla y cajón del Encierro: regiones de Atacama y Coquimbo. Servicio Nacional de Geología y Minería, Carta Geológica de Chile, Serie Geología Básica 175 y 176, 1 mapa escala 1:100.000. Santiago.

Pardo, M., Comte, D. & Monfret, T. (2002) Seismotectonic and stress distribution in the central Chile subduction zone. *J. S. Am. Earth Sci.*, **15**, 11–22.

Pardo-Casas, F. & Molnar, P. (1987) Relative motion of the Nazca plate (Farallon) and South American plates since Late Cretaceous time. *Tectonics*, **6**, 233–248.

Pilger, R. (1984) Cenozoic plate kinematics, subduction and magmatism: South American Andes. *J. Geol. Soc. London*, **141**, 793–802.

Pineda, G. & Emparán, C. (2006). Geología del área Vicuña-Pichasca. Región de Coquimbo. Servicio Nacional de Geología y Minería. Carta geológica de Chile, Serie Geología Básica 97. 1 mapa escala 1:100.000.

Ramos, V. (2010) The tectonic regime along the Andes: Present-day and Mesozoic regimes. *Geol. J.*, **45**, 2–25.

Ramos, V., Cristallini, E. & Pérez, D. (2002) The Pampean flat-slab of the Central Andes. *J. S. Am. Earth Sci.*, **15**, 59–78.

Reutter, K. (1974) Entwicklung und Bauplan der chilenischen Hochkordillere im Bereich 29° südlicher Breite. *Neues Jahrb. Geol. Paleontol. Abh.*, **146**, 153–178.

Riquelme, R., Hérail, G., Martinod, J., Charrier, R. & Darrozes, J. (2007) Late Cenozoic geomorphologic signal of Andean forearc deformation and tilting associated with the uplift and climate changes of the Southern Atacama Desert (26°S-28°S). *Geomorphology*, **86**, 283–306.

Rodríguez, M.P. (2013). *Cenozoic Uplift and Exhumation Above the Southern Part of the Flat-Slab Subduction Segment of Chile (28.5-32°S)*. Tesis para optar al grado de Doctora en Ciencias, mención Geología. Departamento de Geología, Universidad de Chile, Chile.

Rodríguez, M.P., Aguilar, G., Urresty, C. & Charrier, R. (2014) Neogene landscape evolution in the Andes of north-central Chile between 28.5 and 32°S: Interplay between tectonic and erosional processes. *Geol. Soc. Spec. Publ.*, **399**, 419–446.

Rossel, K. (2014) *Estratigrafía y Estudio de Proveniencia de las Sucesiones de Gravas Neógenas en la Cordillera Frontal del Valle del Huasco, Región de Atacama: Formación Laguna Grande (28°45′S)*. Departamento de Geología, Universidad de Chile, Chile, Memoria para optar al título de Geólogo.

Rubatto, D. (2002) Zircon trace element geochemistry: partitioning with garnet and the link between U-Pb ages and metamorphism. *Chem. Geol.*, **184**, 123–138.

Salazar, E. & Coloma, F. (Accepted). Geología del área Cantaritos–Laguna Chica, Región de Atacama. Servicio Nacional de Geología y Minería, Carta Geológica de Chile, Serie Geología Básica. 1 mapa escala 1:100.000. Santiago.

Salazar, E., Coloma, F. & Creixell, C. (2013). Área el Tránsito-Lagunillas, Región de Atacama. Servicio Nacional de Geología y Minería. Carta geológica de Chile, Serie Geología Básica 150. 1 mapa escala 1:100.000. Santiago.

Salfity, A., Gorustovich, S., Moya, M. & Amengual, R. (1984). Marco tectónico de la sedimentación y efusividad cenozoica de la Puna. 9° Congreso Geológico Argentino, pp. 539–554.

Sambridge, M., Braun, J. & McQueen, H. (1995) Geophysical parametrization and interpolation of irregular data using natural neighbours. *Geophys. J. Int.*, **122**, 837–857.

Schildgen, T., Hodges, K., Whipple, K., Reiners, P. & Pringle, M. (2007) Uplift of the western margin of the Andean plateau revealed from canyon incision history, southern Peru. *Geology*, **35**, 523–526.

Schlunegger, F., Kober, F., Zeilinger, G. & von Rotz, R. (2010) Sedimentology-based reconstructions of paleoclimate changes in the Central Andes in response to the uplift of the Andes, Arica region between 19 and 21°S latitude, northern Chile. *Int. J. Earth Sci.*, **99**, 123–137.

Schumm, S., Mosley, M. & Weaver, W. (1987) *Experimental Fluvial Geomorphology*. John Wiley and Sons, New York.

Segerstrom, K. (1963) Matureland of northern Chile and its relationship to ore deposits. *Geol. Soc. Am. Bull.*, **74**, 513–518.

Sempere, T., Hérail, G., Oller, J. & Bonhomme, M. (1990) Late Oligocene-early Miocene major tectonic crisis and related basins in Bolivia. *Geology*, **18**, 946–949.

Sillitoe, R., Mortimer, C. & Clark, A. (1968) A chronology of landform evolution and supergene mineral alteration, southern Atacama Desert, Chile. *Inst. Min. Metall. Transact.*, Section B, **77**, 166–169.

Silver, P., Russo, R. & Lithgow-Bertelloni, C. (1998) Coupling of South American and African Plate Motion and Plate Deformation. *Science*, **279**, 60–63.

Sobel, E., Hilley, G. & Strecker, M. (2003) Formation of internally drained contractional basins by aridity-limited bedrock incision. *J. Geophys. Res.*, **108**, 2344.

Sobolev, S. & Babeyko, A. (2005) What drives orogeny in the Andes? *Geology*, **33**, 617–620.

Somoza, R. (1998) Updated Nazca (Farallon)-South America relative motions during the last 40 My: implications for mountain building in the central Andean region. *J. S. Am. Earth Sci.*, **11**, 211–215.

Steinman, G. (1929) *Geologie von Perú*. Karl Winter, Heidelberg.

Strecker, M.R., Alonso, R., Bookhagen, B., Carrapa, B., Coutand, I., Hain, M.P., Hilley, G.E., Mortimer, E., Schoenbohm, L. & Sobel, E.R. (2009) Does the topographic distribution of the central Andean Puna Plateau result from climatic or geodynamic processes? *Geology*, **37**, 643–646.

Van der Plas, L. & Tobi, A. (1965) A chart for judging the reliability of point counting results. *Am. J. Sci.*, **263**, 87–90.

Willet, S.D., Schlunegger, F. & Picotti, V. (2006) Messinian climate change and erosional destruction of the central European Alps. *Geology*, **34**, 613–616.

Winocur, D., Litvak, V. & Ramos, V. (2014) Magmatic and tectonic evolution of the Oligocene Valle del Cura basin, main Andes of Argentina and Chile: evidence for generalized extension. *Geol. Soc. Spec. Publ.*, **399**, 109–130.

Yáñez, G., Ranero, C., Von Huene, R. & Díaz, J. (2001) Magnetic anomaly interpretation across the southern central Andes (32°-34° S): The role of the Juan Fernandez Ridge in the late Tertiary evolution of the margin. *J. Geophys. Res.*, **106**, 6325–6345.

Yrigoyen, M. (1993). Los depósitos sinorogénicos terciarios. In: *Geología y Recursos Naturales de Mendoza* (Ed. by V. Ramos), pp. 123–148. 12° Congreso Geológico Argentino y 2° Congreso de Exploración de Hidrocarburos (Relatorio 1). Asociación Geológica Argentina, Instituto Argentino del Petróleo, Mendoza.

Zech, R., Kull, C. & Veit, H. (2006) Late Quaternary glacial history in the Encierro Valley, northern Chile (29°S), deduced from ^{10}Be surface exposure dating. *Palaeogeogr. Palaeoclimatol. Palaeoecol.*, **234**, 277–286.

Manuscript received 8 February 2016; In revised form 1 July 2016; Manuscript accepted 13 September 2016.